Final Report: Natural State Models of The Geysers Geothermal System, DOE Contract DE-FG07-98ID13677

T. Brikowski[1], D. Norton[2], D. Blackwell[3]

December 31, 2001

[1]Principal Investigator, Geosciences Program, University of Texas at Dallas, Box 830688, Richardson, TX, 75083, (972) 883-6242, Internet: brikowi@utdallas.edu

[2]Consultant, Stanley, ID, denis@ruralnetwork.net

[3]Subcontractor, SMU, Dallas, TX, blackwel@passion.isem.smu.edu

Contents

List of Figures

1 Introduction

Summarized in the following report are the results obtained in a project focused on natural state (pre-production) modeling of The Geysers geothermal system. The project was motivated by a need to better-understand the origin, current state, and future scenarios for The Geysers to allow better management of this unique energy resource. During the three-year course of the project nine reviewed papers were published, and six oral presentations made to communicate these results to the industrial and academic geothermal communities. Preprints of the papers are attached as appendices, and form the bulk of the material in this report. This introductory section highlights the four most fundamental scientific contributions arising from the project, which are explained more fully in the sections that follow, and are discussed in complete detail in the corresponding publications (appendices).

- Thermal augmentation (e.g. re-intrusion) of the known felsite is required to yield present day temperatures in models of The Geysers, (Brikowski and Norton, 1999; *Norton and Hulen*, 2001, and Appendix B)
- δ^{18}O-alteration generated by the liquid-dominated stage of The Geysers involved relatively low permeability with high horizontal connectivity along the felsite contact (*Brikowski*, 2001b; Brikowski, 2000, and Appendix B)

- Near-critical fluid conditions had a strong impact on the development of The Geysers geothermal system, as evidenced by mineralogic indicators of such conditions in the veins within the hornfels rim of the felsite, supporting the likelihood that near-critical fluid conditions (*Norton et al.*, 2000)

- "Simmering" (development of a mobile transient steam phase) is a dominant state in magma-hydrothermal systems (Brikowski, 2001d, and Appendix E), and probably dominated the early transition to two-phase conditions at The Geysers. Transition to vapor-dominated conditions required reheating of the system no more than 500,000 years ago.

A principal focus of the project has been to understand the importance of supercritical fluid conditions to the development and nature of The Geysers geothermal system. A number of prior studies (*Brikowski*, 2001b; *Brikowski and Norton*, 1989; *Hayba and Ingebritsen*, 1997; *Norton and Knight*, 1977) have demonstrated the important impact that fluid properties have on fluid circulation in such systems, particularly near the fluid critical point (374°C , 22.049 MPa for pure H_2O). Super-critical conditions have been encountered at depth in magmatic geothermal systems (Fig. 1), and are important in the deep conductive zones of non-magmatic system (e.g. U.S. Basin and Range, Wisian, 2000). Natural state models of geothermal systems must necessarily include the heat source, which is generally at or above the critical point of water. Consequently natural state geothermal modeling places a strong emphasis on accurate treatment of near-critical fluid properties. For example, any model that includes the heating zones below production boreholes at The Geysers (black lines, Fig. 1) must be capable of treating supercritical conditions. Model results will be profoundly influenced by those conditions.

The first year of the project was devoted to modeling the liquid-dominated state of The Geysers geothermal system, as constrained by the rock alteration evidence. The next year and a half was dedicated to development and testing of a two-phase, supercritical version of the *TOUGH2* simulator using a new standard H_2O equation of state (*NIST*, 1999), a task that proved far more difficult than anticipated. The final six months of the project were dedicated to applying this new simulator in general studies of the interaction between supercritical heating zones at depth, and two-phase geothermal reservoirs, and preliminary application of these results to analyze the onset of boiling at The Geysers. These final results indicate that development of vapor-dominated conditions was far more complex than previously realized. Considerable modeling and field effort will be needed to properly explore, constrain, and understand this complexity.

2 Liquid-Dominated, δ^{18}O-Calibrated Models

The goal of this task was to gain a regional understanding of the early Geysers fluid circulation system as preserved in the rock alteration record, specifically by the oxygen isotopic alteration described by Moore and Gunderson (1995); Walters *et al.* (1996). Their data in-

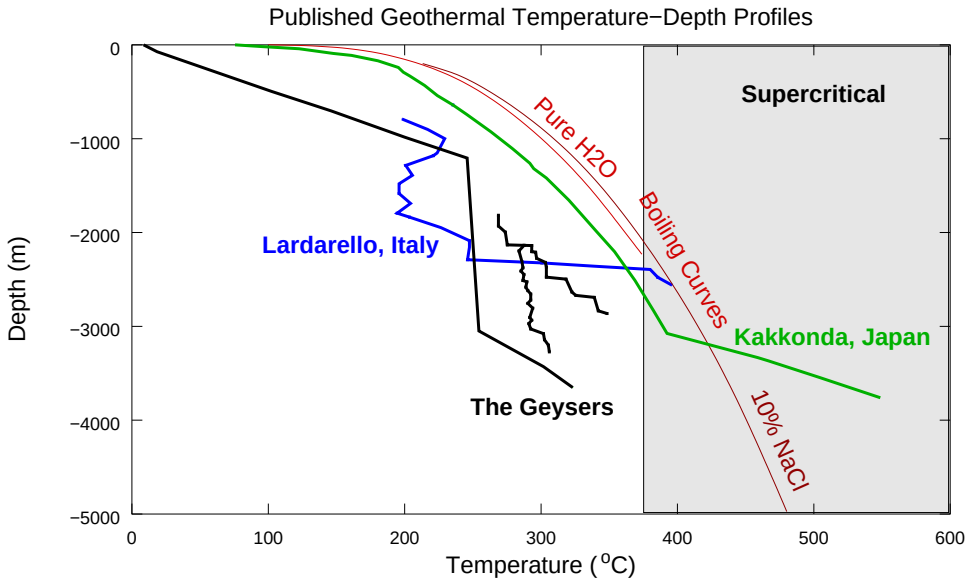

Figure 1: Temperature-depth profiles for high-temperature geothermal systems worldwide (after *Muraoka et al.*, 2000). Observed conditions at the base of these systems exceeds the critical point of water (shaded region). Two-phase boundary (boiling curve) shown in red for pure H_2O and a solution of 10% NaCl.

dicates a somewhat unusual distribution of δ^{18}O alteration low on the flanks of the felsite, in contrast to most hydrothermal systems that develop strong δ^{18}O-depletion above the apex of the magmatic heat source. These models (*Brikowski*, 2001b) used a modified version of an existing computer program (*MARIAH*) to simulate heat, fluid and δ^{18}O-mass transport during the liquid-dominated stage of The Geysers, using observed rock isotopic alteration (Fig. 2) as constraints. For simplicity, modeling was limited to a vertical cross-section extending SW-NE through Geysers coring hole project SB-15d (Fig. 3).

2.1 Principal Conclusions

These models were quite successful in matching the observed alteration, and providing an explanation for the unusual distribution of that alteration at The Geysers (Fig. 4). The limited vertical extent of the zone of maximum δ^{18}O depletion above the flanks of the felsite requires relatively low permeability in the greywacke reservoir (in contrast to the higher permeability required to generate present-day "isothermal" conditions in the reservoir). The position of this zone low on the flanks of the felsite reflects continuous action of a very low permeability cap, probably similar to the present-day lithocap. The horizontally continuous nature of the maximum depletion zone requires good connectivity of permeable zones just above the hornfels region of the intrusion, to allow ready penetration of δ^{18}O-depleted fluids along that zone. The models show progression of an δ^{18}O-alteration front along a stream-tube *parallel* to the felsite contact. Depleted fluids enter the system from the distal margins, reacting with the rock to yield this alteration front. The streamtube, bounded on

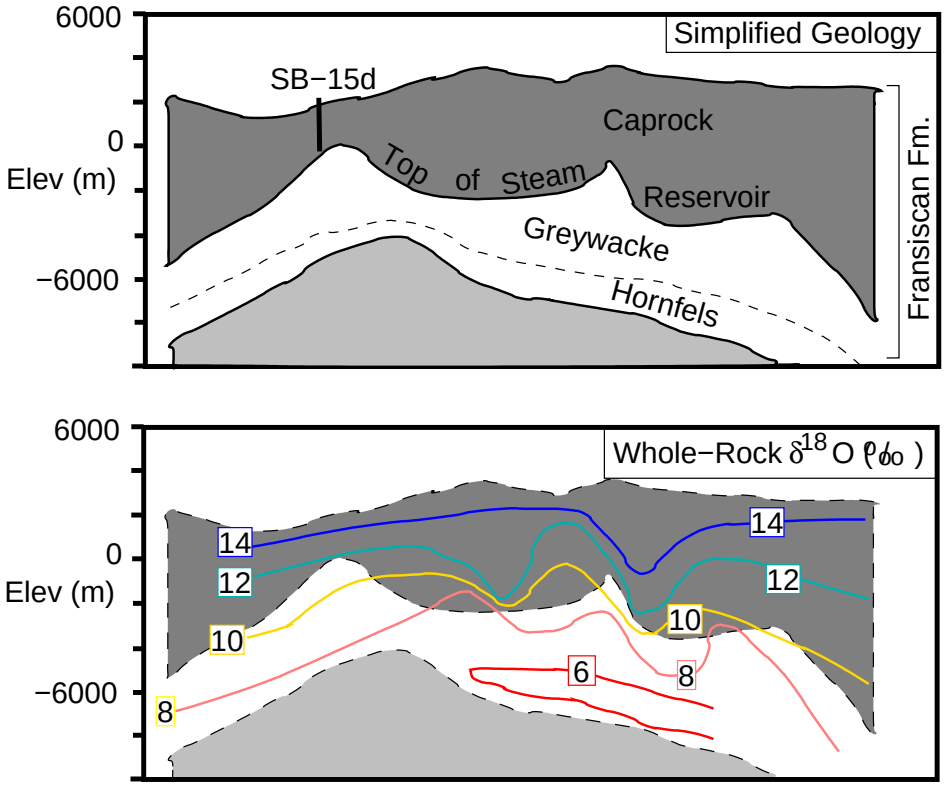

Figure 2: SW-NE cross-section of The Geysers, passing through well SB-15D, showing simplified geology (top, after Hulen *et al.*, 1994) and whole-rock δ^{18}O alteration (bottom, after Moore and Gunderson, 1995) in per-mil (‰). Location of SB-15D and cross-section line shown in Figure 3.

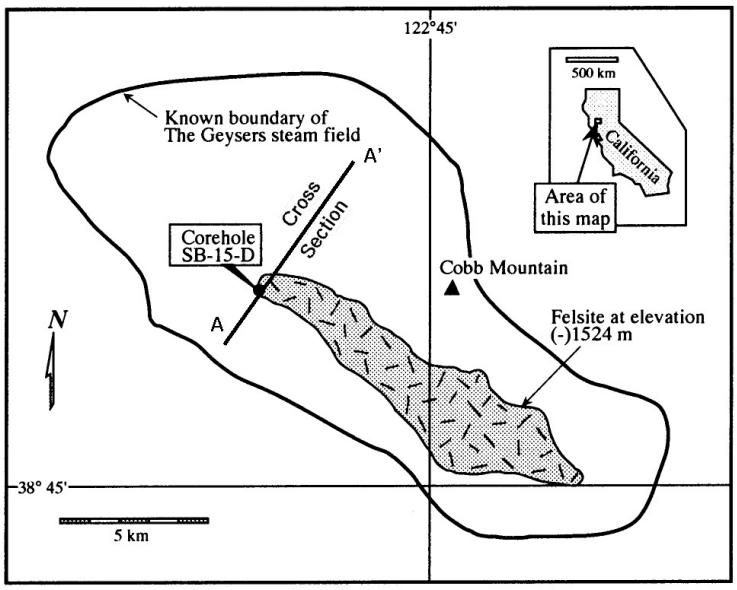

Figure 3: Location of The Geysers steam field, felsite at depth and model cross-section (after Hulen and Moore, 1996) and model cross-section. Coring project well SB-15d and location of model cross-section (A-A') shown near center of steam field.

the bottom by low permeability felsite/hornfels, and on the top by the zone of near-critical fluid conditions, and strongly limits flow to the low flanks of the felsite. See Appendix B for additional details.

These conclusions depart somewhat from the models of Moore and Gunderson (1995); Walters *et al.* (1996), in that these model results require early penetration of depleted formation fluids immediately above the hornfels zone (Fig. 2) along its contact with the greywacke. Also implied by the model results is that hydrothermal generation of secondary porosity (and permeability) in the greywacke reservoir did not occur until after the development of the principal δ^{18}O alteration, probably around 100,000 yr after initial felsite emplacement.

3 Development of a Supercritical Two-Phase Geothermal Simulator

To advance the models to the boiling stage, a new geothermal reservoir simulator was needed that incorporated highly-accurate computation of fluid properties over pressure-temperature ranges from atmospheric to magmatic (whole area of Fig. 33. *HYDROTHERM* (*Hayba and Ingebritsen*, 1997), an available super-critical multi-phase geothermal simulator utilizes smoothed fluid properties, and appears to minimize near-critical effects in order to achieve rapid solution times. Given these constraints and the project goal of examining the combined effects of near-critical and two-phase phenomena in the development of The Geysers,

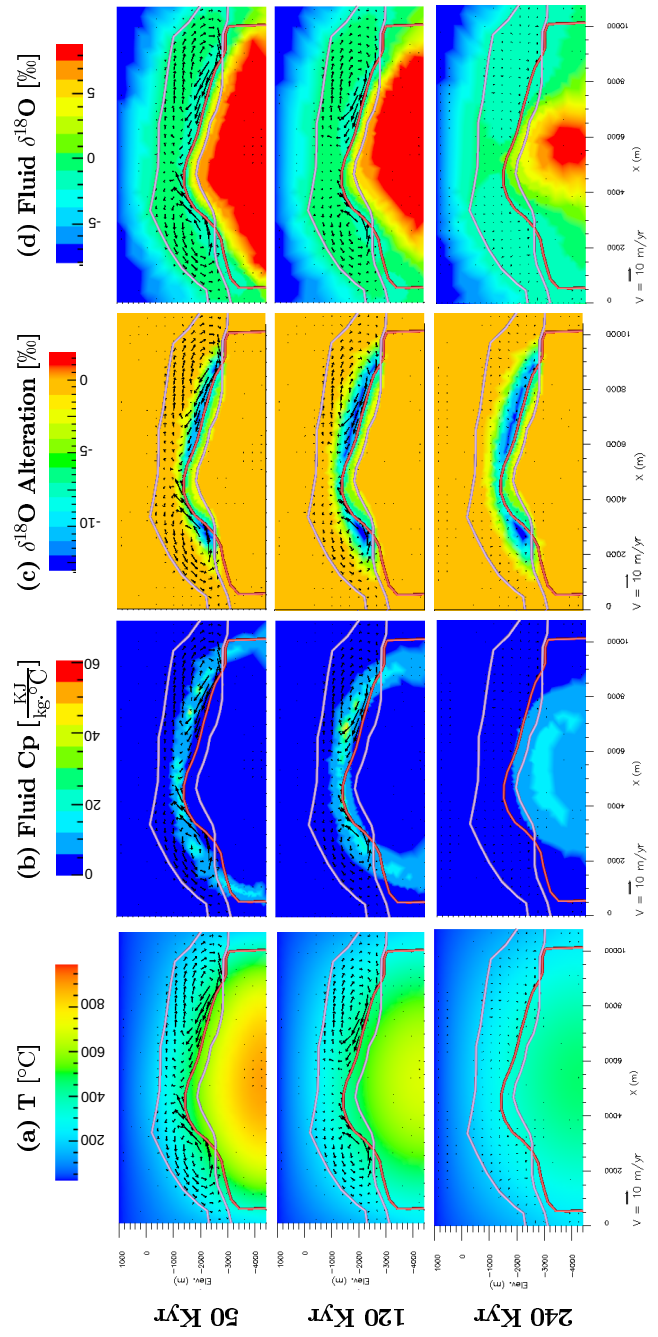

Figure 4: Temperature (column a), fluid heat capacity(b), plagioclase alteration (original minus final composition, column c), and water composition (column d) for 50Kyr, 120Kyr and 240Kyr (rows, in years after felsite intrusion). Shaded contour scales given at top of columns. Black vectors show flow direction, length proportional to velocity; see scale arrow at base of columns. Distance scale given at base of columns, no vertical exaggeration, each panel is 5.4 km deep and 10.8 km wide. Felsite boundary shown by red line, steam reservoir boundary by white lines. Whole rock equivalent alteration is 0.3-0.5 times the values in column (c).

modification of an existing multi-phase heat and mass transport code was deemed to be the most effective approach. *TOUGH2* (*Pruess et al.*, 1999) is the closest to industry-standard geothermal simulator with source code available that treats multi-phase mass (water-steam) and heat flow, but as-distributed is limited to sub-critical conditions (Fig. 33). Initial efforts to modify *TOUGH2* were based on application of the supercritical numerical equation of state (based on NIST equations) developed by *Johnson and Norton* (1991). After much effort, this combination proved unworkable (see discussion *Brikowski*, 2001a,c), and in late May 2001 a numerical equation of state published by the National Institute of Standards (*NIST*, 1999) was adopted instead. This application proved to be successful, and highly-accurate modeling of the onset and evolution of boiling in geothermal systems is now possible. The NIST-based equation of state module has been named *EOS1sc*, reflecting its origins as a modified version of the EOS1 equation of state shipped with *TOUGH2*.

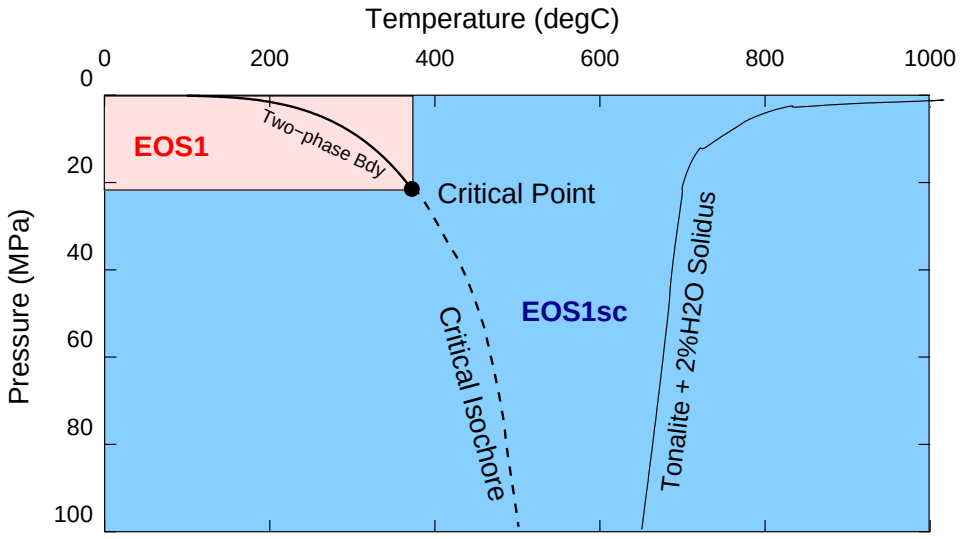

Figure 5: P-T validity ranges of EOS1 (pink shaded area, *Pruess et al.*, 1999) and *EOS1sc* (blue area). Liquid-vapor solidus of hydrous tonalite magma with 2 wt% H_2O shown to indicate typical magmatic conditions (*Whitney*, 1975). Dashed line shows approximate location of critical isochore (line of density equal to density at the critical point).

4 The Onset of Boiling in Generic Models

Preliminary models of the onset of boiling at The Geysers indicated the surprising persistence of simmering (transient steam bubble migration) as the hallmark of that onset (see Appendix E). To better evaluate this process, generic models of magma-hydrothermal systems were carried out to explore the controls on simmering (Brikowski, 2001d). The model system consists of an 0.5x2km pluton, with top 2 km below ground surface and an 0.6 km caprock just below ground surface (Fig. 6). Pressure temperature conditions along a vertical profile through the left-hand column of elements show a rapid evolution to sub-parallel to the two-phase boundary (Fig. 37). The host-rock portion of the profile line is oriented along the

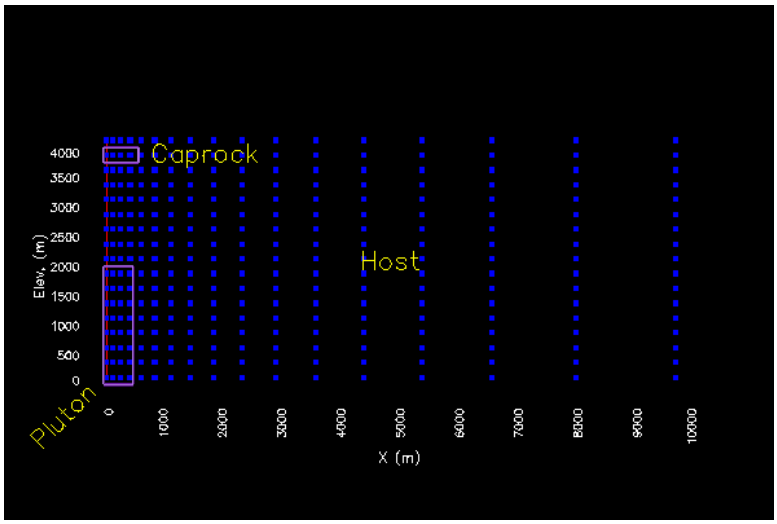

Figure 6: Computational grid and lithologic zones for hypothetical system of caprock, host rock and pluton. Caprock permeability 1.0x10^{-18} m^2, host rock 1.0x10^{-15} m^2, and pluton as 5.0x10^{-17} for temperatures less than the critical point. Profile line (at x=50m) used in subsequent figures shown in red. Grid based on hypothetical model of *Hayba and Ingebritsen* (1997).

principal upflow zone of the system. Those times with extensive zones along the two-phase boundary (2 Kyr and later)are boiling, but not in the steady manner often indicated by two-phase simulators, such as the original *TOUGH2*. A steam phase forms periodically at the base of the upflow zone (nearest to the critical point, Fig. 37), and moves upward with velocity greater than the liquid (i.e. phase separation). These "bubbles" advect upward, to accumulate immediately below the lithocap. Formation of a steam phase at any level in the upflow zone causes overlying points to increase in pressure, and move off the two-phase surface. A complex cycle of oscillatory movement for each node in PT space keeps conditions in the upflow zone just on the liquid side of the two-phase boundary (especially lower portion of 5 Kyr line adjacent to two-phase boundary, Figure 38). This cycle is the manifestation of a powerful feedback system, where in freely-convecting systems heat transport and phase state interact to maintain conditions just to the liquid side of the two-phase boundary. This is the classic definition of simmering, wherein basal heating is dissipated by transient formation and migration of steam bubbles, which are eventually resorbed into the liquid. In most magmatic cooling scenarios in this model geometry, the system never achieves a steady steam phase. Instead simmering persists for most of the hydrothermal lifetime of the system. Pressure perturbations, such as fracturing of the lithocap, are quickly accommodated by the system, and produce only short term changes in steam saturation. Only significant temperature perturbations, such as magma reintrusion, are sufficient to drive the system in to a more steady, vapor-dominated state. Reintrusion serves to drive increased steam production at depth, and increase temperatures throughout the reservoir, and thereby increase steam accumulation and decrease resorbtion at the base of the lithocap.

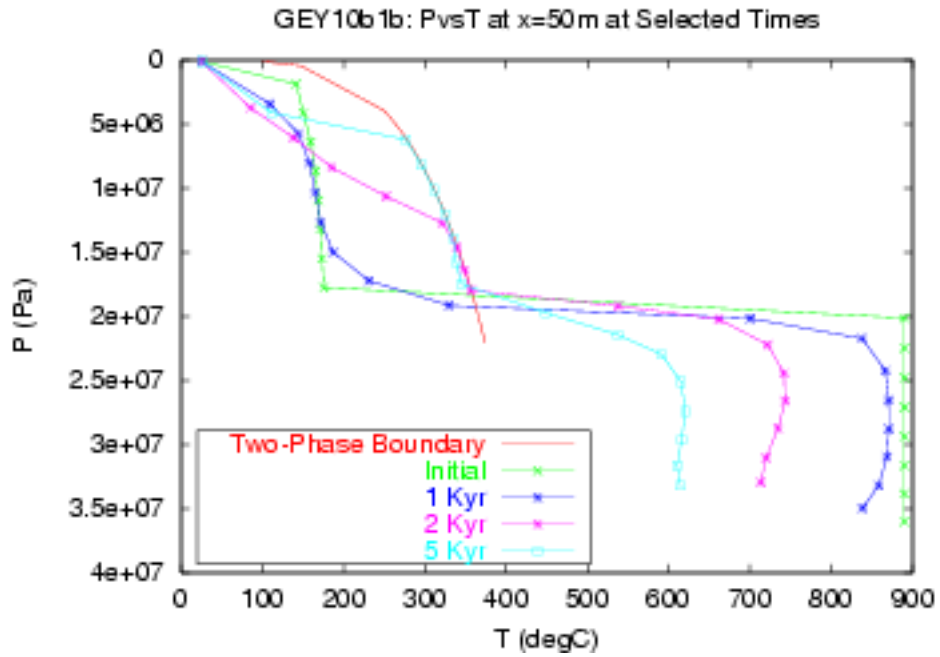

Figure 7: PT profiles along x=50m at selected times. Cell "C" in Figure 38 is the third point from the top on each line.

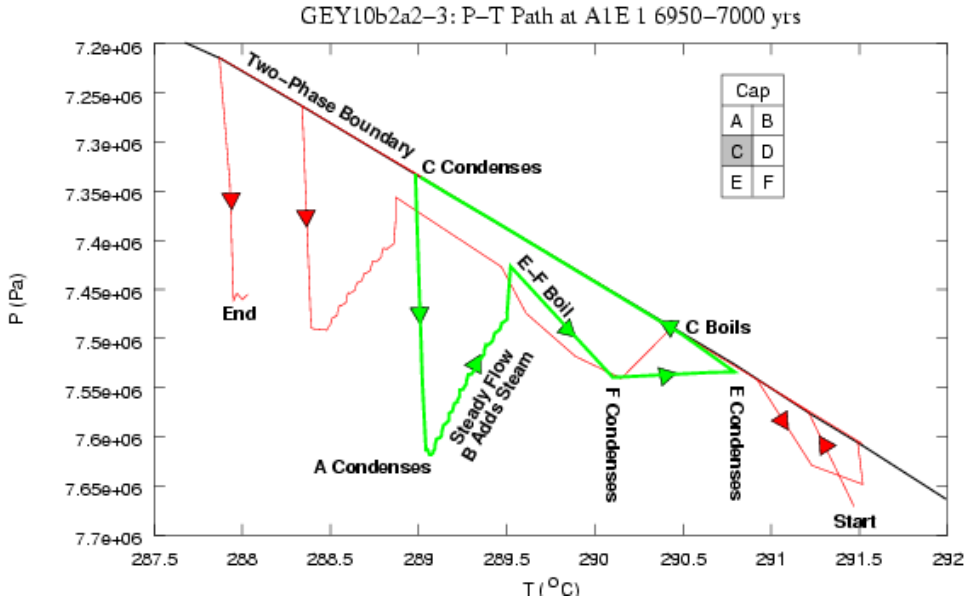

Figure 8: PT history for 100 years at (x,y)=(50,3375)m, designated cell "C" in inset. Neighboring cells are designated by letters given in inset.

4.1 Principal Conclusions

Simmering results have rarely been reported in the past, although simulators such as the unmodified *TOUGH2* do yield such behavior when given proper starting conditions. To generate such behavior requires P-T conditions that roughly parallel the two-phase boundary, and/or its extension past the critical point down the critical isochore (line of density equal to that at the critical point). Magmatic hydrothermal/geothermal systems naturally generate such conditions (e.g. see 1-2Kyr lines, Fig. 37), but models of these systems are unlikely to do so unless supercritical P-T conditions can be treated by the simulator. The stability and likely prevalence of hydrothermal simmering has not been previously recognized because numerical simulations generally did not include natural lower boundary conditions

Simmering models are extraordinarily slow as well. The NIST equation of state is considerably more accurate than the polynomial approximation provided with *TOUGH2*, but requires 10 times more computational effort to determine water properties for each P-T point. In addition, fluid properties reach marked extrema near the critical point; in particular the gradients of fluid density ($\beta = \frac{\partial \rho}{\partial P}$ and $\alpha = \frac{\partial \rho}{\partial T}$ theoretically reach $+\infty$ at the critical point). As points in the numerical solution near the critical point, time step length shrinks to fractions of a year to accommodate the large density changes. Similarly, at lower P-T conditions along the two-phase boundary, the transient appearance and disappearance of a steam phase dramatically changes mass balances at each node, and must be tracked explicitly. This generally holds time steps at 0.1-1 year in length. The net result is that large-scale simmering models using *EOS1sc* are quite computationally intensive, and require long campaigns of model development and completion.

Such behavior has profound implications for our concept of magmatic geothermal systems. Common kitchen experience demonstrates that simmering can be a very stable system state, and only extreme basal heating can move the system into a full boil, or steady two-phase state. In hydrothermal simmering, the development of transient steam zones can dramatically affect local permeability, and clearly perturbs P and T locally. If the process is persistent in nature as it is in models, paleo-indicators of fluid state may only reflect local, very transient conditions. Hydrothermal simmering may explain the complex zonation (e.g. of hornfels tourmalines at The Geysers; *Norton et al.*, 2000) often observed in hydrothermal/geothermal systems, which is generally attributed to tectonic or magmatic processes. In a simmering system, these could just as easily be generated by transient changes in fluid state. See the draft manuscript included as Appendix E for more details, which is planned for submission to AGU journals in early 2002.

5 The Onset of Boiling at The Geysers

Preliminary models of the onset of boiling at The Geysers have been carried out (Appendix E). The models were generated for the The Geysers cross-section utilized in earlier project models (Fig. 3). A finite difference grid of cells 150x250m was utilized (Fig. 9). From the

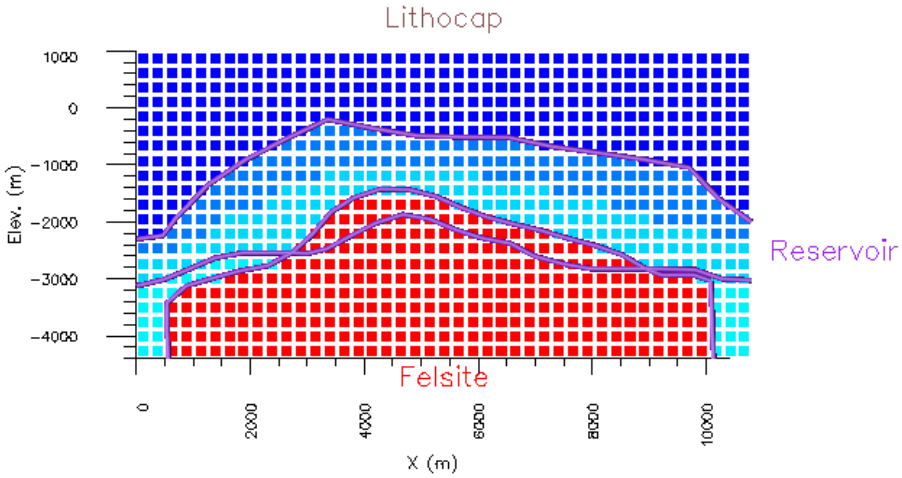

Figure 9: Tough2 Geysers cross-sectional grid. Squares show center of each shell, permeability zones shown in color.

time of magma intrusion the reservoir is assumed to have high permeability (0.1 md) in order to encourage development of an "isothermal" zone as is observed in the present day reservoir. With this assumption, the liquid-dominated stage of the system rapidly evolves into a series of convection cells (Fig. 10). Points in the most vigorous upflow zone, just left of the apex of the intrusion, quickly migrate to form a line along the two-phase boundary and critical isochore over the entire vertical extent of the reservoir (Fig. 11). Note the strong similarity between this upflow zone PT profile and that for the generic model (Fig. 37). In this case, the roots of the upflow zone are at supercritical conditions, and migrate along the critical isochore, past the critical point to lower P-T conditions along the two-phase boundary. At the time shown by the black PT profile (25.6Kyr in this model) steam begins to form at the base of the upflow zone, and convect upward as it did in the generic model. As in the generic model, steam saturations reach no more than 30% (well short of vapor-dominated), and steam zones persist for only 50 years at a time beneath the lithocap.

5.1 Principal Conclusions

At the time of this writing (Oct. 2001) additional models have not been completed, but the lessons from the generic models are clear, development of a vapor-dominated region requires reheating (i.e. magma reintrusion). Simmering persists in the model for at least 100,000 yrs, and it seems likely that reintrusion any time within the period 25000-500000 years after

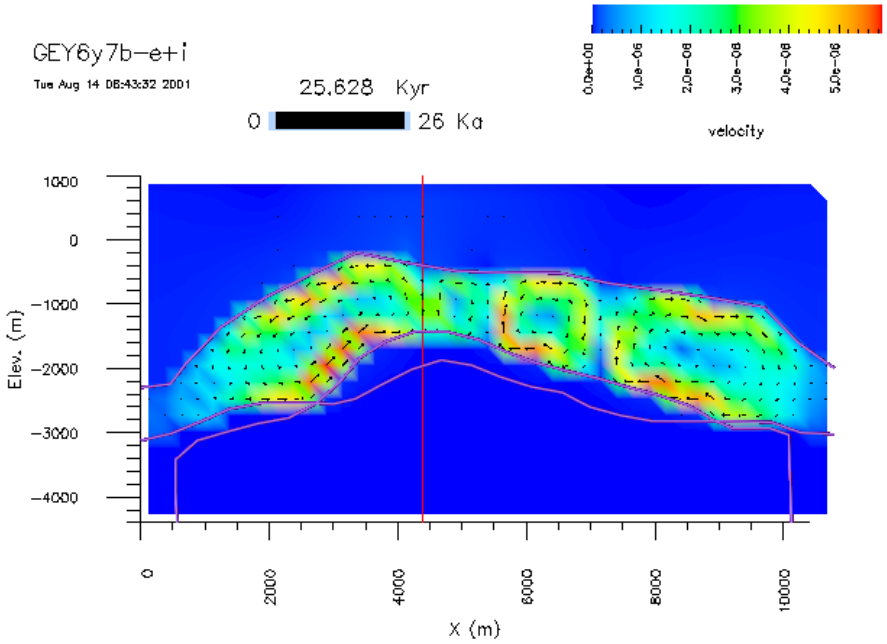

Figure 10: Geysers Tough2 model liquid-dominated stage convection cells. Velocity magnitude shown in color, velocity direction shown by arrows, length proportional to magnitude. Maximum pore velocity 100 $\frac{\text{m}}{\text{yr}}$. Red line shows location of PT profile in Figure 11.

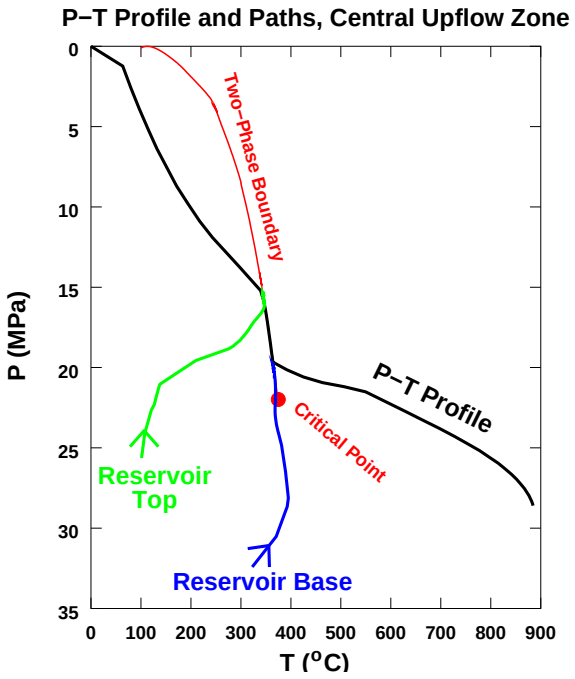

Figure 11: PT paths for vertical profile in primary upflow zone. Profile for 25.6Kyr shown in black, paths labeled by position in reservoir (upflow zone extends from felsite contact to lithocap base). Profile location shown by red line, Figure 10.

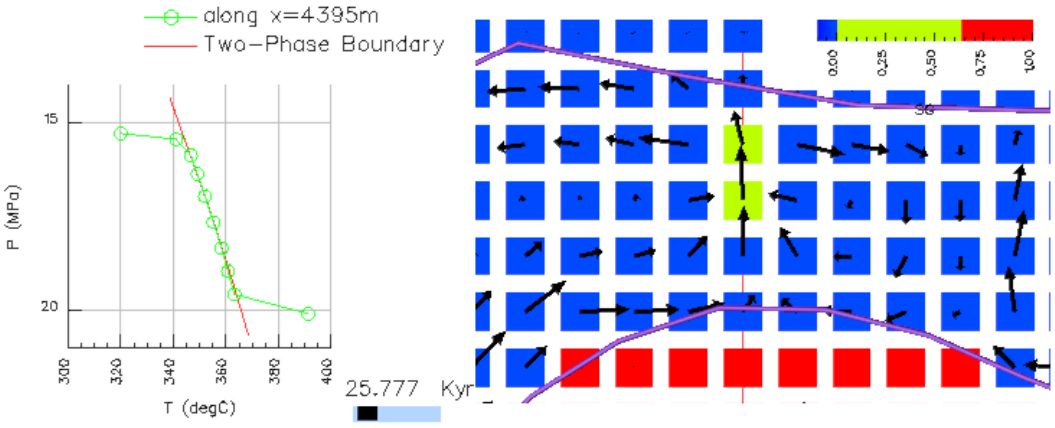

Figure 12: Closeup PT profile and distribution of steam in reservoir portion of primary upflow zone, Geysers Tough2 model at 25.77 Kyr. Steam saturation shown by color, total mass flux (steam+liquid) magnitude and direction shown by vectors, length proportional to magnitude.

initial intrusion of felsite would produce the vapor-dominated system we see today. It is important to note that in a system with supercritical roots, hydrothermal simmering is the predominant process for enhanced heat transport. Mechanisms such as the heat pipe of Pruess (1985) do not function in a simmering environment. In effect high temperatures at the base of the system force a more gently dipping PT profile in upflow zones, making vaporstatic pressure distributions (typical of heat pipe zones) unlikely during the growth of boiling. The heat pipe may be important during retrograde cooling of the system, serving to enhance and maintain vapor-dominated conditions, and in fact it may be such a mechanism that finally pushes the system into a vapor-dominated state.

6 Summary

One of the initial motivations of this project was to generate more realistic starting conditions for present-day production models of The Geysers, in order to allow prediction of sustainable management strategies for the field. This is an identified weakness of current models (Williamson, 1990). In an unanticipated way, the project succeeded in that endeavor. The persistence of simmering in magma-hydrothermal/geothermal systems was unrecognized prior to this study, and indicates that pre-development distribution of steam saturation is likely to have been quite transient and unpredictable if The Geysers heating came from a single intrusion. If instead reintrusion has taken place, as required by conductive models (*Norton and Hulen*, 2001) and certainly convective models (Brikowski, 2000; *Brikowski*, 2001b), pre-development steam saturation would primarily be a function of caprock geometry and distribution of major fracture zones. In any case, long term persistence of simmering phenomena in geothermal systems, particularly The Geysers means that petrologic evidence such as fluid inclusion analysis may give only a snapshot of a highly heterogeneous and transient fluid phase. On the other hand, steam-generated fracturing may have been focused by this process, leading to long-term stability of upflow zones even after production began. In a system where secondary porosity is so important, the feedback-stabilized nature of simmering may have been crucial in determining the present-day distribution of permeability at The Geysers.

Easily the most significant result to emerge from this project is the demonstration that under the conditions most often thought to exist at depth in magmatic geothermal systems, simmering is a very stable state. This concept should seem reasonable to anyone who has boiled water on a stove. The likelihood that hydrothermal simmering is the most common state of two-phase systems means that current interpretation of the significance most mineralogic and geochemical PT indicators must be reconsidered. Conversely details of mineralogic and vein zoning may yield invaluable information about the range of simmering variability (i.e. the cycles shown in Fig. 38), and therefore about conditions throughout the simmering column (at least for upflow zones). *Individual* PT measurements may reflect only local, transient states of the system. The *range* of such measurements at one location may constrain conditions over a much broader area, since a persistent simmering state would allow projection of PT conditions up or down the flow direction. In any case, variability in

the rock record of hydrothermal/geothermal systems may be caused strictly by fluid property variations during simmering, and may not require or constrain any outside processes such as tectonic fracturing.

References

Brikowski, T. H., 2000. Using isotopic alteration modeling to explore the Natural State of The Geysers geothermal system, USA. In: Proceedings of the World Geothermal Congress, pp. 2045–50, kyushu-Tohoku, Japan.

Brikowski, T. H., 2001a. Deep fluid circulation and isotopic alteration in The Geysers geothermal system: Profile models. Geothermics 30 (2-3), 333–47, URL http://www.utdallas.edu/~brikowi/Research/Geysers/Geothermics2K/.

Brikowski, T. H., 2001b. Modeling Supercritical Systems With Tough2: Preliminary Results Using the EOS1sc Equation of State Module. In: Proceedings: Twenty-Sixth Workshop on Geothermal Reservoir Engineering, Stanford University, Stanford, CA, vol. 26 of *SGP-TR-168*, p. 8, URL http://www.utdallas.edu/~brikowi/Research/Geysers/Stanford2001/geysers_stanford01.pdf.

Brikowski, T. H., 2001c. Modeling Supercritical Systems With Tough2: The EOS1sc Equation of State Module and a Basin and Range Example. In: Geother. Resources Council Transact., Geothermal Resources Council, Davis, CA, vol. 25, pp. 285–289, URL http://www.utdallas.edu/~brikowi/Research/Geysers/GRC01/grc01_paper.pdf.

Brikowski, T. H., 2001d. The onset of hydrothermal boiling: Simmering as a persistent state in hydrothermal/geothermal systems. Geophys. Research Lett. 29, 22, URL http://www.utdallas.edu/~brikowi/Research/Geysers/JGR01/jgr01_paper.pdf, to be submitted in early 2002.

Brikowski, T. H., Norton, D., 1989. Influence of magma chamber geometry on hydrothermal activity at mid-ocean ridges. Earth Planet. Sci. Lett. 93, 241–255.

Brikowski, T. H., Norton, D., 1999. An isotope-calibrated natural state model of The Geysers geothermal system: Initial results. Geotherm. Resour. Council Transact. 23, 347–350.

Hayba, D. O., Ingebritsen, S. E., 1997. Multiphase groundwater flow near cooling plutons. J. Geophys. Res. 102 (6), 12235–12252.

Hulen, J. B., Koenig, B., Nielson, D. L., 1994. The Geysers coring project a cooperative investigation of reservoir controls in a vapor dominated geothermal system. Geotherm. Resour. Council Transact. 18, 317–323.

Hulen, J. B., Moore, J. N., 1996. Secondary mineralogy and oxygen-isotope geochemistry of two peripheral steam-exploration boreholes at The Geysers geothermal field, California. Geotherm. Resour. Council Transact. 19, 451–456.

Johnson, J. W., Norton, D., 1991. Critical phenomena in hydrothermal systems: State thermodynamic, electrostatic, and transport properties of H_2O in the critical region. Am. J. Sci. 291, 541–648.

Moore, J. N., Gunderson, R. P., 1995. Fluid inclusion and isotopic systematics of an evolving magmatic-hydrothermal system. Geochim. et Cosmo. Acta 59 (19), 3887–3908.

Muraoka, H., Yasukawa, K., Kimbara, K., 2000. Current state of development of deep

geothermal resources in the world and implications to the future. In: Iglesias, E., Blackwell, D., Hunt, T., Lund, J., Tmanyu, S. (eds.), Proceedings of the World Geothermal Congress 2000, International Geothermal Association, pp. 1479–1484.

NIST, 1999. NIST/ASME STEAM PROPERTIES DATABASE: VERSION 2.2. NIST Standard Reference Database 10, U.S. National Institute of Standards and Testing, URL http://www.nist.gov/srd/nist10.htm.

Norton, D., Hulen, J., Dutrow, B., 2000. Patterns of dynamical hydrothermal activity in geothermal resources, special Progress Note, submitted to U.S. DOE Office of Geothermal and Wind Technologies.

Norton, D., Knight, J., 1977. Transport phenomena in hydrothermal systems: Cooling plutons. Am. J. Sci. 277, 937–981.

Norton, D. L., Hulen, J. B., 2001. Geologic Analysis and Thermal-History Modeling of The Geysers Magmatic-Hydrothermal System. Geothermics 30 (2-3), 211–234.

Pruess, K., 1985. A quantitative model of vapor dominated geothermal reservoirs as heat pipes in fractured porous rocks. Geotherm. Resour. Council Transact. 9, 353–361.

Pruess, K., Oldenburg, C., Moridis, G., 1999. TOUGH2 User's Guide, Version 2.0. Report LBNL-43134, Lawrence Berkeley Nat. Lab, Berkeley, CA.

Walters, M. A., Moore, J. N., Nash, G. D., Renner, J. L., 1996. Oxygen Isotope Systematics and Reservoir Evolution of the Northwest Geysers, CA. Geotherm. Resour. Council Transact. 20, 413–421.

Whitney, J. A., 1975. The effects of pressure, temperature and χ_{H_2O} on phase assemblage in four synthetic rock compositions. J. Geol. 83, 1–31.

Williamson, K. H., 1990. Reservoir simulation of The Geysers geothermal field. In: Proceedings, 15th Workshop on Geothermal Reservoir Engineering, Stanford Univ., Stanford, CA, vol. SGP-TR-130, pp. 113–123.

Wisian, K. W., 2000. Insights into Extensional Geothermal Systems from Numerical Modeling. Geotherm. Resour. Council Transact. 24, 281–286.

A Delivered Project Results

In the course of this project, the following items were produced as part of technology transfer and communication to industry and the scientific community.

- Ten Scientific Papers (reviewed)

Oct. 1999 Brikowski, T. H., Norton, D., 1999, An isotope-calibrated natural state model of The Geysers geothermal system: Initial results. Geotherm. Resour. Council Transact. 23, 347-350.

June, 2000 Brikowski, T. H., 2000, Using isotopic alteration modeling to explore the Natural State of The Geysers geothermal system, USA. In: Proceedings of the World Geothermal Congress, pp. 2045-50, Kyushu-Tohoku, Japan.

Oct. 2000 Wisian, K. W., 2000. Insights into Extensional Geothermal Systems from Numerical Modeling. Geother. Resources Council Transact., Geothermal Resources Council, Davis, CA, vol. 24, p. 281-286 (also presented at World Geothermal Congress, June 2000)

Jan. 2001 Brikowski, T. H., 2001, Modeling Supercritical Systems With Tough2: Preliminary Results Using the EOS1sc Equation of State Module. In: Proceedings: Twenty-Sixth Workshop on Geothermal Reservoir Engineering, Stanford University, Stanford, CA, vol. 26 of SGP- TR-168, p. 8

March 2001 Deep fluid circulation and isotopic alteration in The Geysers geothermal system: Profile models. Geothermics 30(2-3), 333-47.

March 2001 Norton, D. L., Hulen, J. B., 2001, Geologic Analysis and Thermal-History Modeling of The Geysers Magmatic-Hydrothermal System. Geothermics 30(2-3), 211-234.

Sept. 2001 Brikowski, T. H., 2001c, Modeling Supercritical Systems With Tough2: The EOS1sc Equation of State Module and a Basin and Range Example. Geother. Resources Council Transact., Geothermal Resources Council, Davis, CA, vol. 25, pp. 285-289.

Sept. 2001 Wisian, K. W., D. D. Blackwell and M. Richards, 2001. Correlation of surface heat loss and total energy production for geothermal systems. Geother. Resources Council Transact., Geothermal Resources Council, Davis, CA, vol. 25, p. 331-336

Nov. 2001 Brikowski, T. H., 2002, The onset of hydrothermal boiling: Simmering as a persistent state in hydrothermal/geothermal systems. Geophys. Research Lett., v. 29, 22 p., to be submitted Dec. 2001.

- Other Reports

March 2000 Brikowski, T. H., D. Norton and D. Blackwell, 2000. Natural state models of The Geysers geothermal system, Sonoma County, California. DOE Program Review.

March 2000 Brikowski, T. H. An internet-based 3D interactive model of The Geysers geothermal system. Online version of this model available at http://www.utdallas.edu/~brikowi/Research/Geysers/VRML/vbdetect_geysers_view.html.

Dec. 2000 Norton, D., Hulen, J., Dutrow, B., 2000, Patterns of dynamical hydrothermal activity in geothermal resources. Special Progress Note, submitted to U.S. DOE Office of Geothermal and Wind Technologies.

- Presentations

Oct. 20, 1999 Brikowski, T. H., Norton, D., 1999, An isotope-calibrated natural state model of The Geysers geothermal system: Initial results. Geotherm. Resour. Council Annual Meeting, Reno, NV. An online version of the presentation slides is available at http://www.utdallas.edu/~brikowi/Research/Geysers/GRC99_Talk/geyTalk.html.

June 2, 2000 Brikowski, T. H., 2000, Using isotopic alteration modeling to explore the Natural State of The Geysers geothermal system, USA. World Geothermal Congress, Kyushu-Tohoku, Japan. An online version of the presentation slides is available at http://www.utdallas.edu/~brikowi/Research/Geysers/WGC2K/wgc2k_talk_final.pdf.

Jan. 20, 2001 Brikowski, T. H., 2001, Modeling Supercritical Systems With Tough2: Preliminary Results Using the EOS1sc Equation of State Module. Twenty-Sixth Workshop on Geothermal Reservoir Engineering, Stanford University, Stanford, CA. An online version of the presentation slides is available at http://www.utdallas.edu/~brikowi/Research/Geysers/Stanford2001/stanford01_talk_final.pdf.

Aug. 28, 2001 Brikowski, T. H., 2001, Modeling Supercritical Systems With Tough2: Investigating The Onset of Boiling at The Geysers. Geother. Resources Council Annual Meeting, San Diego, CA. An online version of the presentation slides is available at http://www.utdallas.edu/~brikowi/Research/Geysers/GRC01/grc01_talk_final.pdf.

B Preprint: 2001 Geothermics Geysers Special Volume Paper

Deep Fluid Circulation and Isotopic Alteration in The Geysers Geothermal System: Profile Models

Tom Brikowski
Geosciences Department FO-21, University of Texas at Dallas, P.O. Box 830688, Richardson, TX 75083-0688

Abstract

Rock alteration patterns related to the large felsic intrusive complex (felsite) beneath The Geysers steam field (California, USA) are important indicators of the origins of the modern geothermal system. Metagreywacke host rocks for the system show widespread moderate oxygen isotope alteration in the permeable steam reservoir above the felsite, with concentrated alteration low on the flanks of the intrusion. Numerical models of fluid, heat and oxygen isotope transport in the pre-development (natural state) Geysers system demonstrate that an unbroken caprock is required throughout

the liquid-dominated lifetime of the system to produce this pattern. The widespread moderate alteration throughout the steam reservoir suggests a long-lived liquid system, and probably required upwardly increasing permeability in the steam reservoir. The models indicate the maximum hydrothermal lifetime for the system is 0.5 million years (Myr), whereas the youngest dated large intrusive is 1.2 Myr. Combined, these factors indicate repeated igneous intrusions at The Geysers, up to at least 0.5-0.6 Myr ago, and development of a stable liquid-dominated system after that, the evolution of which was truncated by a relatively recent transition to vapor-dominated conditions. Observed chemical compartmentalization of fluids in The Geysers steam reservoir is inconsistent with the lateral extensiveness of alteration at depth, since the latter requires good horizontal connectivity of deep permeable zones to allow penetration of ^{18}O-depleted fluids. This compartmentalization is probably recent, developing as a consequence of vapor-dominated conditions introducing relative permeability effects. Petrologic evidence for high paleo-fluid temperatures (300°C) within 1 km of the surface is difficult to reconcile with subdued ^{18}O alteration beneath these locations. These peak paleotemperatures are likely to indicate small, short-lived penetrations of the caprock. Natural-state models allow the combined influence of these factors on the evolution of The Geysers to be analyzed quantitatively. Internet-accessible graphical animations of these results are available at http://www.utdallas.edu/~brikowi/Research/Geysers.

Nomenclature

English Symbols	Meaning	Units
$A,\ B$	parameters in isotope exchange equilibrium constant formula	
C_i	chemical concentration (mass per unit volume of ^{18}O in phase i)	-
C_p	isobaric heat capacity	$\frac{\text{J}}{\text{kg}^{\circ}\text{C}}$
$\mathbf{D}$	dispersion coefficient tensor	$\frac{\text{m}^2}{\text{sec}}$
k_{if}	kinetic exchange constant between phase i and fluid	$\frac{1}{\text{sec}}$
R	$^{18}\text{O}/^{16}\text{O}$ ratio	-
T	temperature	°C
$\vec{q}$	Darcy vector velocity	m/sec
t	time	sec
Greek Symbols		
α_{if}	isotopic fractionation factor between i and fluid	-
Δ_{if}	equilibrium isotopic fractionation between phases i and fluid	‰
$\delta^{18}\text{O}_i$	normalized isotopic ratio in phase i	‰
ν	atomic mass fraction of oxygen	-
ϕ_i	volume fraction of i-th phase	-
ρ_i	density of i-th phase	$\frac{\text{kg}}{\text{m}^3}$
Subscripts	Meaning	
r	rock phase property	
f	fluid phase property	

B.1 Introduction

The Geysers offer a unique opportunity in the U.S. to study an active hydrothermal system where the plutonic heat source can be sampled directly. An overview and synthesis of system characteristics can be developed by employing system-wide fluid mass and heat balances in space and time to generate natural state models of its evolution. Such models can provide the broad understanding of The Geysers needed for sustainable management of the geothermal resource based on fundamental physical and thermodynamic principles. This paper describes results of fluid and heat flow models for the liquid-dominated state of The Geysers, including quantitative constraints on the hydrothermal system derived from vein-mineral geothermometry and observed rock isotopic alteration. The analysis begins from a geologically known condition, the initial appearance of the heat source (magma intrusion). From this starting condition, the models calculate the dissipation of the original thermal and chemical energy of the intrusion into its host rocks. Temperature, pressure, fluid flow and chemical composition (δ^{18}O) fields are computed for The Geysers hydrothermal system from the time of its inception to a time immediately prior to the onset of vapor-dominated conditions. These models are also constrained (calibrated) using the current state of the system, including the temperature and pressure fields, distribution of chemical and isotopic alteration, and distribution of fractures and permeability. Since the liquid phase is most efficient at isotopic alteration, observed alteration provides strong direct constraints on the liquid-dominated state of The Geysers, and indirect constraints on the modern vapor-dominated system.

The Geysers may best be viewed as a plutonic hydrothermal system that has been profoundly affected by shallow depth of intrusion and low-permeability host rocks. The Geysers exhibit many of the features found in fossil plutonic hydrothermal systems, including development of a low-permeability caprock above a more permeable altered zone. Strong alteration at The Geysers is concentrated low on the flanks of the underlying intrusive (Moore and Gunderson, 1995). This is in sharp contrast to the typical mushroom-shaped alteration zones found above the center of the intrusive heat source in numerical (Brikowski, 1995; Norton and Taylor, 1979) and conceptual models of magma-hydrothermal systems (e.g. copper porphyry systems, Gustafson and Hunt, 1975). The models below focus on prediction and analysis of the temporal and spatial distribution of oxygen isotope alteration at The Geysers. These results are then used to characterize the dominant processes influencing the evolution of the liquid-dominated stage of The Geysers geothermal system.

B.1.1 Geologic Setting

The Geysers (Fig. 13) is one of a few productive vapor-dominated systems in the world, and currently produces approximately 1036 MWe (Calpine Inc., 2000) from a 75 km^2 area (Walters and Combs, 1992). The system has been extensively explored and developed, with data available from some 780 deep wells, many penetrating the underlying plutonic heat source. The Geysers system is developed in a structurally complex collection of Jurassic to Creta-

ceous metamorphic rocks, primarily metagreywacke, assigned to the Franciscan Assemblage (Fig. 14). Pleistocene intrusion of felsic rocks, collectively termed "felsite" (Hulen and Nielson, 1996; Schriener and Suemnicht, 1980; Thompson, 1992), provided the heat and reservoir permeability for the system. The main body of the felsite intrusive is found as shallow as 0.7 km depth below the present surface in the southeastern Geysers, with minimum radiometric ages of around 1.2 Ma (Dalrymple *et al.*, 1999; Hulen *et al.*, 1997). The geometry of the felsite top is relatively well characterized, and has been described in a variety of publications (Hulen *et al.*, 1994; Hulen and Walters, 1993, Norton and Hulen, this volume, Fig. 2). Permeability was generated in the roof rocks of the intrusive by hydrothermal dissolution of earlier metamorphic vein carbonate (Hulen and Nielson, 1995), and thermally-driven hydraulic fracturing (Norton and Hulen, this volume). A caprock is present, distinguished by undissolved metamorphic calcite and younger vein-filling calcite apparently related to the modern hydrothermal system. This system has left a strong alteration and metasomatic signature, forming a distinctive tourmaline-bearing biotite hornfels along the contact of the felsite, and marked depletion of whole rock δ^{18}O along the lower flanks of the felsite (Fig. 14, lower portion).

B.1.2 Model Scenario

In order to study general aspects of the development of this complex, active, and incompletely characterized system, a number of simplifying assumptions were adopted. System permeability was assumed to be purely a function of lithology, and invariant with time. The present-day distribution of the steam reservoir (i.e. zone of borehole steam entries) was used as an initial estimate of the distribution of caprock and permeable zones above the felsite. The impact of through-going fault zones was assumed to be minimal in the models. Modern fluid isotopic and non-condensable gas compositions have been cited as evidence of compartmentalization (i.e. fault zones forming impermeable barriers) between the Northwestern and main Geysers steam reservoirs (Truesdell *et al.*, 1995; Walters *et al.*, 1996). The area chosen for modeling is well south of these proposed barriers. The felsite was treated as a single, instantaneous intrusion, with no additional heat input into the system.

The models aim to match observed alteration and paleotemperature indicators. Petrologic constraints on paleotemperatures are available from drilled core and cuttings (Hulen *et al.*, 1997; Hulen and Nielson, 1995; Moore *et al.*, 1989). Moore and Gunderson (1995) have outlined the distribution of δ^{18}O alteration at The Geysers, finding an 8‰ decrease in rock δ^{18}O along the felsite-greywacke contact (Fig. 14), and a 4–6‰ decrease throughout the rest of the steam reservoir. Similar observations have been made for the Northwest Geysers (Walters *et al.*, 1996). Isotopic alteration was assumed to occur via diffusive exchange. Isotopic exchange rates were assumed to be functions of temperature and initial lithology, the transient effects of mineral dissolution, precipitation and mineral surface area changes were neglected. These assumptions are consistent with field evidence for lack of wholesale recrystallization or dissolution/replacement of minerals in the reservoir rocks.

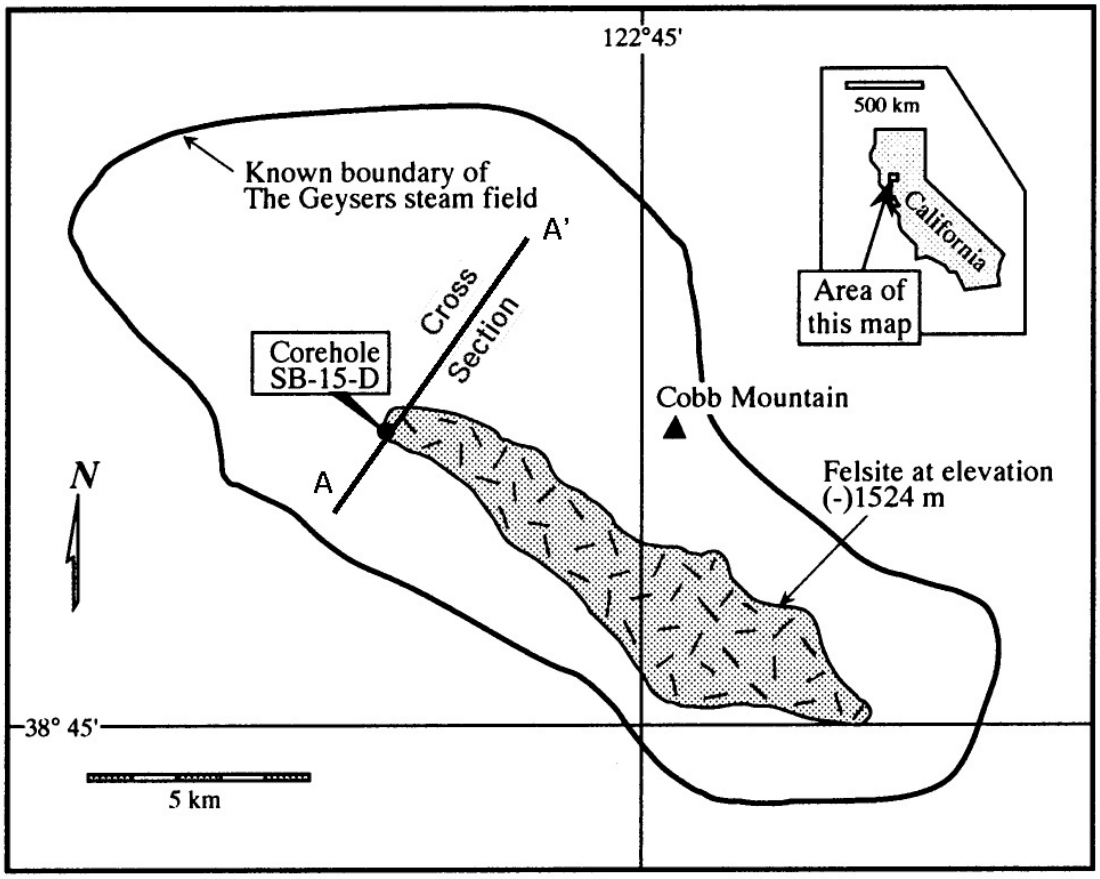

Figure 13: Location of The Geysers steamfield, felsite and model cross-section (after Hulen and Moore, 1996). Coring project well SB-15D and location of model cross-section (A-A', see also Norton and Hulen, this volume) shown near center of steam field.

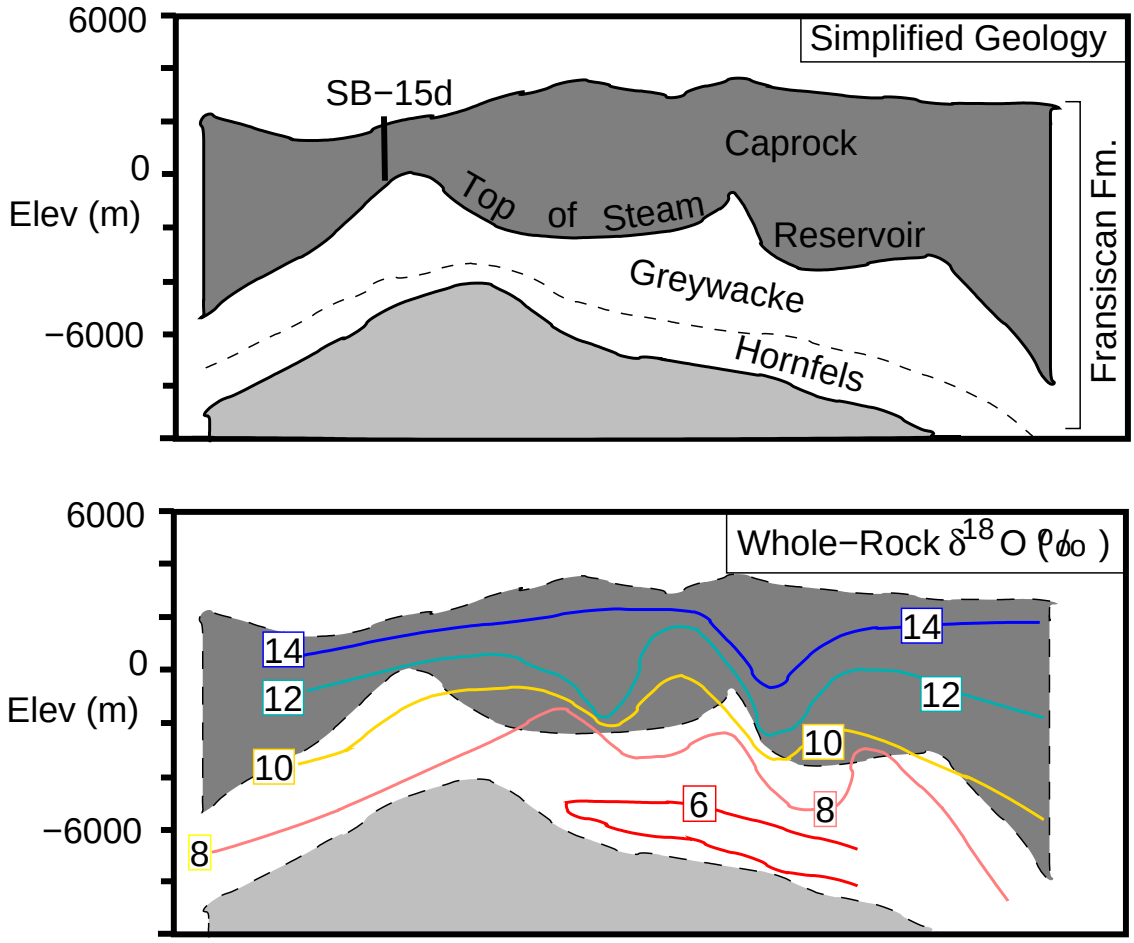

Figure 14: SW-NE cross-section of The Geysers, passing through well SB-15D, showing simplified geology (top, after Hulen *et al.*, 1994) and whole-rock δ^{18}O alteration (bottom, Moore and Gunderson, 1995) in per-mil (‰). Location of SB-15D and cross-section line shown in Figure 13.

B.1.3 Model Geometry

Modeling was carried out in cross-section, identical in location to that of several earlier studies (Brikowski and Norton, 1999, Norton and Hulen, this volume). Those studies investigated the basic time and length scales for hydrothermal circulation at The Geysers using system-wide mass and heat balances, implemented via relatively coarse finite difference models of heat and fluid flow. The models in this study build on the results of those preliminary analyses, obtaining solutions of heat, fluid and isotope transport using a detailed finite element discretization (Fig. 15) of the same section (Fig. 14). The two-dimensional cross-sectional grid is oriented SW-NE passing through Geysers Coring Project well SB-15D, and extending 10.8 km horizontally and 5.4 km vertically (see line, Fig. 13). Permeability zones were based on current distributions of steam reservoir and felsite (Fig. 14); a single instantaneous intrusion of granodiorite at temperature 975°C was assumed for the heat source. Initial host rock temperatures followed a $40\frac{^\circ\mathrm{C}}{\mathrm{km}}$ geotherm. Caprock thickness was increased 20% over present values to account for erosion. Consequently, boiling conditions were not present in the reservoir and felsite in this model.

B.2 Governing Equations

The governing relationships for heat and fluid transport are well established, and will not be reviewed here (e.g. *Norton and Knight*, 1977; *Pruess et al.*, 1999). Isotope transport can be modeled using the standard advection-dispersion equation, modified to utilize a suitable chemical concentration variable and appropriate treatment of chemical reaction. These modifications are detailed below.

Many solutions to the simplified isotope transport equation are expressed in terms of rock isotopic ratio $R \equiv {}^{18}\mathrm{O}/{}^{16}\mathrm{O}$. For example Cook and Bowman (1994) use such an approach to constrain ratios of transport parameters based on observed alteration profiles. The models described below were developed in terms of $\delta^{18}\mathrm{O}$ (isotope ratio R normalized to a standard) in order to simplify comparison to observations reported as $\delta^{18}\mathrm{O}$. A similar derivation is made by Norton and Taylor (1979). For simplicity, rock reaction is treated as exchange between the fluid and a single solid phase. The advection-dispersion equation (i.e. mass balance for ${}^{18}\mathrm{O}$) for such system can be written as (Bear, 1979, eqn. 7-42):

$$\underbrace{\frac{\partial(\phi\rho C)_f}{\partial t}}_{\text{Liquid Composition}} = \underbrace{-\nabla\cdot[\phi_f \mathbf{D}\nabla(\rho C)_f]}_{\text{Dispersion/Diffusion}} - \underbrace{\nabla[\vec{q}(\rho C)_f]}_{\text{Advection}} - \underbrace{\frac{\partial(\phi\rho C)_r}{\partial t}}_{\text{Rock Composition}} \tag{1}$$

where C_i is the chemical concentration (mass per unit volume of ${}^{18}\mathrm{O}$ in phase i), ϕ_i and ρ_i are the volume fraction and density of phase i, $\mathbf{D}$ is the dispersion coefficient tensor, and $\vec{q}$ is the fluid Darcy velocity. The concentration variable can be expressed in detail using the definition of $\delta^{18}\mathrm{O}$:

$$C_i = \nu_i\left(\frac{\delta^{18}\mathrm{O}_i}{10^3} + 1\right)\cdot R_{standard} \tag{2}$$

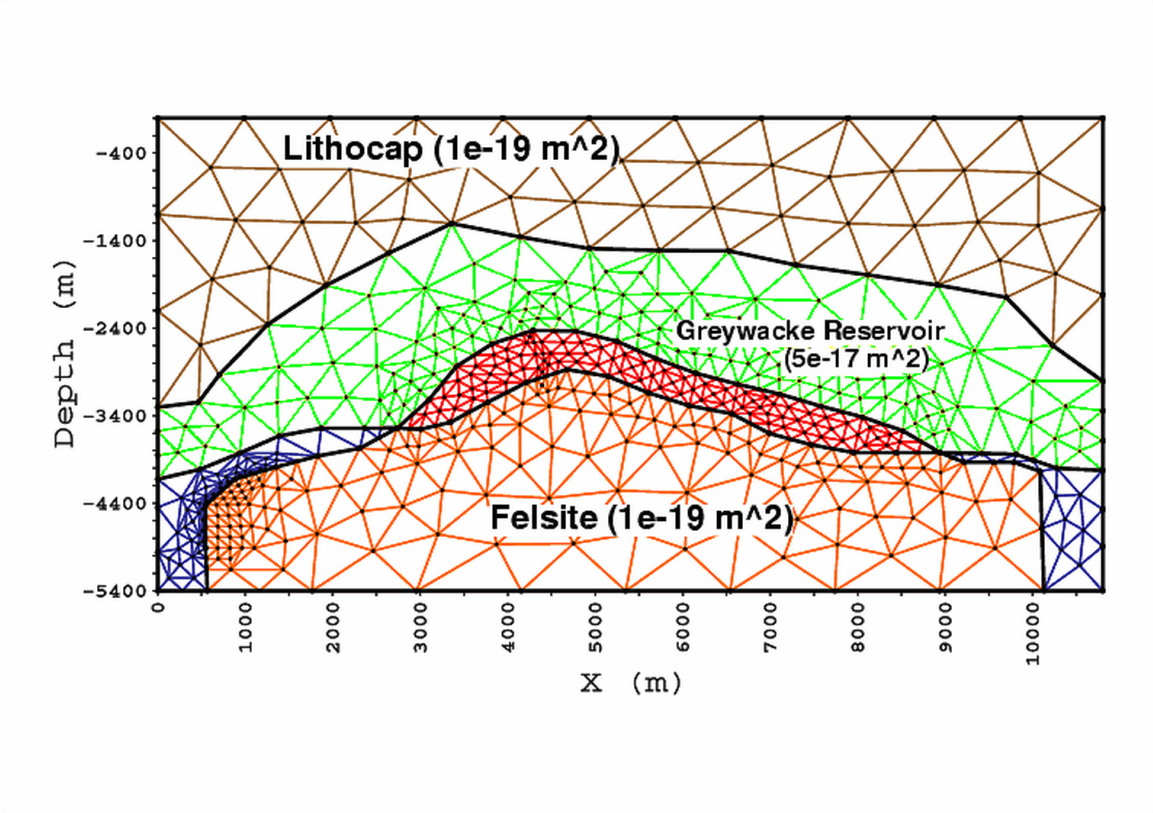

Figure 15: Finite element model grid, showing lithologic zones and modeled intrinsic permeability. Permeable reservoir boundaries shown by thick line (includes some felsite lithology), felsite boundary shown by thinner solid line (i.e. area of initially-hot rock). Bottom of well SB-15D is located approximately at the highest point of the steam reservoir-caprock contact. The model contains 1071 quadratic triangular elements and 2188 nodes.

where ν_i is the mass of exchangeable oxygen in phase i. Then (1) can be rewritten as:

$$\frac{\partial(\phi\rho\nu\delta^{18}\mathrm{O})_f}{\partial t} = \nabla\cdot[\mathbf{D}\nabla(\phi\rho\nu\delta^{18}\mathrm{O})_f] \;-\; \nabla[\vec{q}(\rho\nu\delta^{18}\mathrm{O})_f] - \frac{\partial(\phi\rho\nu\delta^{18}\mathrm{O})_r}{\partial t} \tag{3}$$

The equation describing rock composition as a function of water-rock exchange of ^{18}O in a system is assumed to follow a first-order rate law (Gregory *et al.*, 1989, eqns. 9-10):

$$\frac{\partial R_i}{\partial t} \;=\; k_{if}\Big(\underbrace{\alpha_{if}R_f}_{\text{equilibrium } R_i} \;-\; \underbrace{R_i}_{\text{actual } R_i}\Big) \tag{4}$$

where k_{if} is the kinetic exchange coefficient between mineral i and the fluid (units $\frac{1}{\text{sec}}$), modeled using an Arrhenius relationship (i.e. thermally activated, Cole and Ohmoto, 1986). This can be converted to δ notation by observing that:

$$\delta_i^{18(eq)} = \delta^{18}\mathrm{O}_f \;+\; \Delta_{if}$$
$$\Delta_{if} \equiv \frac{A_i}{T^2} + B_i$$

where Δ_{if} is the equilibrium isotopic compositional difference between phase i and fluid (expressed in δ notation), T is temperature in °C , A_i and B_i are tabulated fit parameters to laboratory data for phase i (e.g. Bottinga and Javoy, 1973). Then (4) becomes:

$$\frac{\partial\delta^{18}\mathrm{O}_i}{\partial t} \;=\; k_{if}(\delta^{18}\mathrm{O}_f \;+\; \frac{A}{T^2} \;+\; B \;-\; \delta^{18}\mathrm{O}_i) \tag{5}$$

which describes the change in δ^{18}O with time in the ith reacting mineral in the volume of interest. Since Δ_{if} is the equilibrium δ^{18}O difference between mineral i and fluid at current temperature and pressure, exchange between minerals and fluid is proportional to the reaction rate (which is strongly proportional to temperature) and the compositional difference between the current assemblage and a hypothetical one at equilibrium. Equation (5) describes the source/sink term in the standard advection-dispersion equation for transport of ^{18}O. Assuming a single reacting phase (i.e. substitute r for i), and substituting that expression for the right hand term of (4) obtains the final form for the ^{18}O mass conservation equation used in this study:

$$(\nu\phi)_f\frac{\partial(\rho\delta^{18}\mathrm{O})_f}{\partial t} \;=\; \nabla\cdot\mathbf{D}\nabla(\nu\phi\rho\delta^{18}\mathrm{O})_f \;-\; \vec{v}\cdot\nabla(\nu\rho\delta^{18}\mathrm{O})_f - (\nu\phi\rho)_r\; k_{rf}(\delta^{18}\mathrm{O}_f + \frac{A_r}{T^2} + B_r - \delta^{18}\mathrm{O}_r) \tag{6}$$

This equation can be solved using finite difference or element methods. For this study, a much-modified version of the finite-element program Mariah (Brikowski, 1995; *Brikowski and Norton*, 1989) was used to model the system governed by this and the heat and fluid flow equations.

B.3 Model Results

Two-dimensional models of heat and fluid flow and ^{18}O transport were made using a finite element model over the cross-section depicted in Figure 14. To allow for maximum solution stability, grid density was concentrated where high advection and reaction rates were anticipated (Fig. 15). The top boundary of the model was held at constant temperature and pressure, model sides and base were treated as impermeable and insulating. Owing to distal deepening and constriction of the reservoir, the choice of permeable or impermeable side conditions had little effect on the solution. Repeated model runs were made, adjusting parameters (calibrating) until an adequate fit was achieved to observed $\delta^{18}O$ alteration, geothermometers, and general constraints on surficial heat flow in the system. Details of the transfer function for isotopic exchange between fluid and mineral are poorly constrained (e.g. reactive mineral surface area), and therefore the results should be viewed in terms of average transfer rate. In fact this approach to model calibration leads to good constraints on time-integrated ratios of reaction to advection (Damkohler number) and diffusion to advection (Peclet number) rather than the values of the individual parameters making up those ratios.

B.3.1 Heat Transport and Fluid Convection

The model results demonstrate a number of fundamental features of The Geysers hydrothermal system. Perhaps of greatest significance are constraints on system lifetime. Purely conductive models of the geometry shown in Figure 15 indicate a maximum lifetime of 0.7 Myr (this study and Norton and Hulen, this volume), convective models using the indicated permeabilities reduce this lifetime to 0.35-0.5 Myr (Fig. 4a, lifetime defined as the time at which fluid velocity declines to $\leq 1 \frac{\text{cm}}{\text{yr}}$ throughout the reservoir). The youngest date available for the main felsite body is 1.18 Myr (Dalrymple *et al.*, 1999; Hulen *et al.*, 1997). This discrepancy indicates that The Geysers natural state system has had a considerably more complicated intrusive and hydrothermal history than is generally assumed. Similar conclusions have been reached by other authors based on geophysical analysis (Stanley and Blakely, 1995) and crustal-scale conductive thermal models (Dalrymple *et al.*, 1999).

Convection in the system is tightly restricted along the upward-sloping flanks of the felsite (vectors, Fig. 4). The lower boundary of this flow zone is controlled by the permeability contrast between reservoir and "basement felsite" rocks. The upper margin of this zone is formed by localization of near-critical fluid properties. Recall that heat transport and fluid flow properties reach extrema near the fluid's critical point (374°C and 22 MPa for pure water). These properties are computed in the model using an accurate numerical equation of state (*Johnson and Norton*, 1991). Heat capacity displays a sharp peak vs. temperature and pressure, reaching $+\infty$ at the critical point, providing a useful indicator of near-critical conditions. A mantle of near-critical conditions develops in the host rock in the vicinity of the 375°C temperature contour (Fig. 4b). This contour moves outward from the felsite until around 125 thousand years (Kyr), at the peak of hydrothermal activity, and then slowly

retreats downward. By 240 Kyr critical conditions are within the deep, low-permeability felsite, and effective (liquid) hydrothermal circulation ceases in the system. Hydrothermal circulation above the apex of the felsite is limited by the presence of the caprock, requiring divergent flow in that area, and by sub-critical fluid conditions within the greywacke reservoir there. Influx of formation water into the system is tightly channeled by these two phenomena, and is localized deep on the flanks of the intrusive. The net result of the permeability and fluid property variations is to develop two circulation cells centered low on the flanks of the intrusive. Influx of fluid into these cells is from the distal portions of the steam reservoir, discharge is into the upper central steam reservoir. Models with permeable sides for the reservoir showed little difference, owing to the narrowing and deepening of the reservoir at the model boundaries, limiting horizontal fluid flow. In this single convecting phase model the system transports heat primarily by conduction after about 250 Kyr. Reservoir temperatures remain greater than present-day values (235 °C) until around 400 Kyr.

B.3.2 Transport Model

To investigate the alteration impacts of this localized convection, the ^{18}O transport equation (6) was solved simultaneously with the heat and fluid transport equations. For simplicity, a single reactant mineral was assumed, effectively treating the system as two phases (liquid and solid) with only isotopic exchange and fluid advection allowed as chemical transfer mechanisms. In this way a bulk or equivalent transfer coefficient is obtained through model calibration, which reflects the combined influence of multiple exchanging minerals in the rock, of transient changes in mineralogy and reactive mineral surface area. The transfer direction and rate are treated as functions of temperature and phase composition. Parameters for the rate law were derived from the following considerations. Average groundmass mineralogy of The Geysers host rock metagreywacke is approximately 40% quartz, 30% plagioclase and 30% illite+chlorite (Moore and Gunderson, 1995). Lambert and Epstein (1992) note limited reaction of quartz grains in the greywacke, which suggests that the primary reactant mineral in isotope exchange is plagioclase. Volume fraction of plagioclase in rock was assumed to be 0.30, and volume fraction of mobile water in rock ϕ_f =1.0x10^{-3}. Isotopic parameters are the water-plagioclase isotope fractionation factor A = 2.61x10^6 and B = -3.7 (Bottinga and Javoy, 1973). Parameters for the Arrhenius formulation of the kinetic exchange coefficient were activation energy ΔE = 20000 $\frac{\text{cal}}{\text{mole}}$, pre-exponential factor A_o = 1.0x10^{-6} $\frac{1}{\text{sec}}$. These values are consistent with averages summarized in Cole and Ohmoto (1986) and Lasaga (1981). The formulation gives an effective maximum transfer rate in the models of approximately 10^{-7} $\frac{\text{moles O}}{\text{m}^3 \text{ sec}}$, equivalent to 2.5–2.5x10^4 one cm^3 plagioclase crystals per m^3 rock at maximum reaction rates (5.5x10^{-5}–5.5x10^{-9} $\frac{\text{moles O}}{\text{m}^2 \text{ sec}}$, Cole and Ohmoto, 1986). Dispersion coefficient was set to 10^{-7} $\frac{\text{m}^2}{\text{sec}}$. Grid Courant number was maintained $\leq$ 1. Streamline upwinding was used in the finite element model to obtain a convergent solution under these conditions.

Alteration in the system begins quickly, with notable rock alteration visible by 20Kyr. By 50Kyr, depleted fluids have penetrated much of the way up the flanks of the felsite (top

image, Fig. 4d). Because temperatures are high, rapid isotopic exchange is taking place, and the alteration progresses as a reaction front up the stream tube formed by the permeability contrast and critical-properties zone (Fig. 4b). Isotopically depleted fluids enter this tube in the deep, distal part of the model. As fluids progress through the tube, approach the apex of the system and moving more sluggishly, they become enriched in δ^{18}O via exchange with the rock and no longer produce noticeable alteration (Fig. 4b). Had the caprock been permeable above the apex of the felsite, very strong convection would take place in that area, and a marked plume of ^{18}O–depleted fluids would alter the rocks in a vertical zone above the apex. The lack of such a pattern argues strongly for the presence of an unbroken caprock throughout the effective liquid hydrothermal lifetime of The Geysers system. Although some vein materials from corehole SB-15D support high fluid temperatures at the top of the reservoir, this is not consistent with the lack of strong ^{18}O depletion in the shallow reservoir. Instead it seems that the SB-15D veins record small short-lived zones of penetration of the caprock.

These alteration models, based as they are on a simplified view of The Geysers setting, do not completely match the observed moderate alteration throughout the reservoir (Hulen *et al.*, 1994; Moore and Gunderson, 1995). One possible model adjustment is to assume a larger kinetic factor k_{rf}, however doing so results in retrograde alteration (i.e. moderate re-enrichment of rock) by late-stage enriched fluids in the models. While retrograde mineralogic overprint has been invoked in porphyry systems (e.g. the "phyllic overprint" of Gustafson and Hunt, 1975), petrologic evidence for this in The Geysers reservoir rocks is negligible. The Arrhenius parameters used in the models shown here limit significant isotopic exchange to areas with temperature ≥ 400°C , whereas the upper portions of the reservoir reach a maximum of 300°C in a region where Hulen *et al.* (1994) show whole rock depletion of 4-6 ‰. A possibility is that a larger kinetic factor is more appropriate, with the development of two-phase conditions (boiling) in the reservoir soon after maximum temperatures were reached, preventing retrograde alteration. A more probable alternative is that higher permeability in the upper reservoir led to higher fluid temperatures, allowing more complete isotopic exchange. Further modeling is underway to explore this alternative. In particular, the constant permeability assumed for the reservoir in the above models contrasts with observations of decreasing reservoir porosity (and presumably permeability) with depth (Gunderson, 1990). Monotonically increasing permeability with distance from the felsite may provide a better match to observed alteration.

B.4 Conclusions

This initial analysis of the natural state of The Geysers, constrained in particular by observed δ^{18}O alteration reveals a number fundamental features of the system:

- low bulk permeabilities in the reservoir rock (0.05 md) are sufficient to allow the convective circulation of fluids required to produce observed alteration and vein mineralogies. These values are in general agreement with those determined in two-phase models of

The Geysers steam reservoir (Pham and Menzies, 1993; Williamson, 1990), indicating that the reservoir permeability during the liquid-dominated phase of The Geysers was similar to present-day values.

- effective liquid hydrothermal circulation (given those permeabilities) persists for only 300 Kyr after a single intrusion with the known geometry of the felsite.
- reservoir temperatures remain above present day values for only 400 Kyr after magma intrusion
- enhanced heat and fluid transport related to critical fluid properties strongly focuses inflow and deep fluid convection into a "streamtube" along the felsite-greywacke contact.
- isotopic rock alteration is strongly limited to the recharge zones of this streamtube, and becomes much weaker in the discharge zone of the streamtube near the apex of the felsite; hence maximum alteration is observed low on the flanks of the intrusive.
- persistent integrity of the caprock is required to produce this pattern of flow and resulting alteration. Without the caprock, a vertical zone of strong isotopic alteration should be present above the apex of the felsite, a zone which is not apparent in the data of Moore and Gunderson (1995).
- persistent horizontal hydraulic connectivity at depth is also required to preserve the streamtube effect along the low flanks of the felsite intrusive. Present-day inferred barriers to horizontal mixing of reservoir fluids were apparently inactive during the liquid-dominated stage of The Geysers.
- widely distributed moderate alteration within the reservoir supports one of several alternatives:
  - a long-lived liquid-dominated system developed (probably maintained by repeated igneous intrusions), with boiling occurring soon after maximum temperatures were reached
  - temperature-controlled deposition of minerals reduced permeability close to the felsite between 20-100Kyr, allowing longer term alteration of the upper steam reservoir
  - more than one intrusive and hydrothermal episode produced the observed isotopic alteration at The Geysers

The limited thermal lifetimes demonstrated here strongly indicate that the intrusive history of the felsite heat source at The Geysers is more complex than indicated by available radiometric dates. The rest of the features itemized above are related to the limited fluid circulation at The Geysers, which is responsible for the unusual thermal and alteration structure above the intrusive. Consideration of system-wide heat, fluid mass and ^{18}O mass

balances at The Geysers allows a fundamental understanding of these features, and provides new insights regarding The Geysers, as well as a firm basis for more focused reservoir engineering and production models.

B.5 Acknowledgements

Geological and geochemical insights from Jeff Hulen, EGI, and Denis Norton, Stanley ID, were crucial in generating and improving these models. Several anonymous reviewers provided comments that greatly improved the manuscript. This research supported by the Assistant Secretary for Energy Efficiency and Renewable Energy, Geothermal Division, U. S. Dept. of Energy under contract DE-FG07-98ID13677.

References

Bear, J., 1979. Hydraulics of Groundwater. McGraw-Hill, New York, NY.

Bottinga, Y., Javoy, M., 1973. Comments on oxygen isotope geothermometry. Earth. Plan. Sci. Lett. 20, 250–65.

Brikowski, T. H., 1995. Isotope-calibrated hydrothermal models: Geothermal implications of a model of the Skaergaard Intrusion. Geotherm. Resour. Council Transact. 19, 171–176.

Brikowski, T. H., Norton, D., 1989. Influence of magma chamber geometry on hydrothermal activity at mid-ocean ridges. Earth Planet. Sci. Lett. 93, 241–255.

Brikowski, T. H., Norton, D., 1999. An isotope-calibrated natural state model of The Geysers geothermal system: Initial results. Geotherm. Resour. Council Transact. 23, 347–350.

Calpine Inc., 2000. The Geysers/The Hill Headlines. (map), 50 West San Fernando Street, San Jose, California 95113.

Cole, D. R., Ohmoto, H., 1986. Kinetics of isotopic exchange at elevated temperatures and pressures. Reviews in Mineralogy 16, 41–90.

Cook, S. J., Bowman, J. R., 1994. Contact metamorphism surrounding the Alta stock: Thermal constraints and evidence of advective heat transport form calcite + dolomite geothermometry. Am. Mineral. 79, 513–525.

Dalrymple, G. B., Grove, M., Lovera, O. M., Harrison, T. M., Hulen, J. B., Lanphere, M. A., 1999. Age and thermal history of the Geysers plutonic complex (felsite unit), Geysers geothermal field, California: a $^{40}Ar/^{39}Ar$ and U-Pb study. Earth Plan. Sci. Lett. 173 (3), 285–298.

Gregory, R. T., Criss, R. E., Taylor, H. P., 1989. Oxygen isotope exchange kinetics of mineral pairs in closed and open systems: Applications to problems of hydrothermal alteration of igneous rocks and precambrian iron formations. Chem. Geol. 75, 1–42.

Gunderson, R. P., 1990. Porosity of reservoir graywacke at The Geysers. Geotherm. Resour. Council Trans. 14, 1661–65.

Gustafson, L. B., Hunt, J. P., 1975. The porphyry copper deposit at El Salvador, Chile. Econ. Geol. 70, 856–912.

Hulen, J. B., Heizler, M. T., Stimac, J. A., Moore, J. N., Quick, J. C., 1997. New constraints

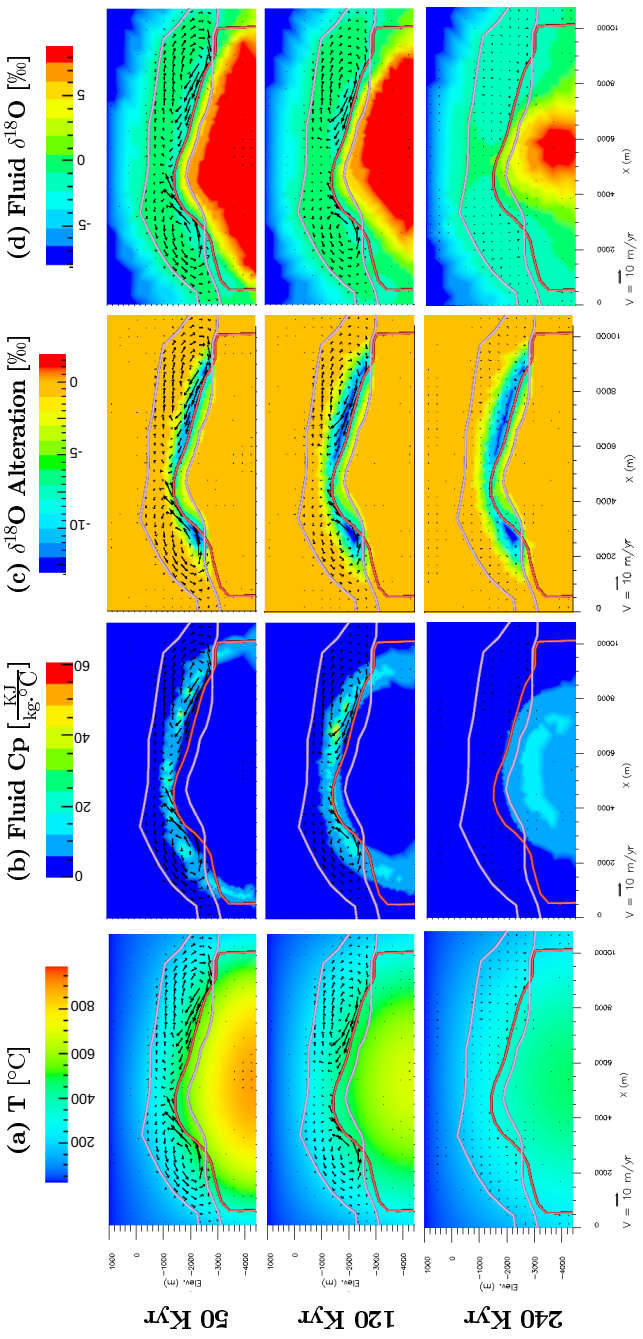

Figure 16: Temperature (column a), fluid heat capacity(b), plagioclase alteration (original minus final composition, column c), and water composition (column d) for 50Kyr, 120Kyr and 240Kyr (rows, in years after felsite intrusion). Shaded contour scales given at top of columns. Black vectors show flow direction, length proportional to velocity; see scale arrow at base of columns. Distance scale given at base of columns, no vertical exaggeration, each panel is 5.4 km deep and 10.8 km wide. Felsite boundary shown by red line, steam reservoir boundary by white lines. Whole rock equivalent alteration is 0.3-0.5 times the values in column (c).

on the timing of magmatism volcanism, and the onset of vapor-dominated conditions at The Geysers steam field, California. In: Workshop on Geothermal Reservoir Engineering Proceedings, Stanford Geothermal Program, vol. 22, pp. 75–82.

Hulen, J. B., Koenig, B., Nielson, D. L., 1994. The Geysers coring project a cooperative investigation of reservoir controls in a vapor dominated geothermal system. Geotherm. Resour. Council Transact. 18, 317–323.

Hulen, J. B., Moore, J. N., 1996. A Comparison of Geothermometers for The Geysers Coring Project, California - Implications for Paleotemperature Mapping and Evolution of The Geysers Hydrothermal System. Geotherm. Resour. Council Transact. 20, 307–314.

Hulen, J. B., Nielson, D. L., 1995. Hydrothermal factors in porosity evolution and caprock formation at The Geysers steam field, California, insight from The Geysers coring project. Stanford Geotherm. Pgm. Proceed. 20, 91–98.

Hulen, J. B., Nielson, D. L., 1996. The Geysers Felsite. Geotherm. Resour. Council Transact. 20, 295–306.

Hulen, J. B., Walters, M. A., 1993. The Geysers felsite and associated geothermal systems, alteration, mineralization, and hydrocarbon occurrences. In: Rytuba, J. J. (ed.), Active geothermal systems and gold-mercury deposits in the Sonoma-Clear Lake volcanic fields, California, Soc. Econ. Geol., vol. 16 of *Guidebook Series*, pp. 141–152.

Johnson, J. W., Norton, D., 1991. Critical phenomena in hydrothermal systems: State thermodynamic, electrostatic, and transport properties of H_2O in the critical region. Am. J. Sci. 291, 541–648.

Lambert, S. J., Epstein, S., 1992. Stable-isotope studies of rocks and secondary minerals in a vapor-dominated hydrothermal system at The Geysers, Sonoma County, California. J. Volc. Geotherm. Res. 53, 199–226.

Lasaga, A. C., 1981. Transition state theory. Reviews in Mineralogy 8, 135–69.

Moore, J. N., Gunderson, R. P., 1995. Fluid inclusion and isotopic systematics of an evolving magmatic-hydrothermal system. Geochim. et Cosmo. Acta 59 (19), 3887–3908.

Moore, J. N., Hulen, J. B., Lemieux, M. M., Sternfield, J. N., Walters, M. A., 1989. Petrographic and fluid inclusion evidence for past boiling, brecciation, and associated hydrothermal alteration above the Northwest Geysers steam field, California. Geotherm. Resour. Council Transact. Geother. Resour. Council, 467–472.

Norton, D., Knight, J., 1977. Transport phenomena in hydrothermal systems: Cooling plutons. Am. J. Sci. 277, 937–981.

Norton, D. L., Taylor, H. P., 1979. Quantitative simulation of the hydrothermal systems of crystallizing magmas on the basis of transport theory and oxygen isotopes data: An analysis of the Skaergaard Intrusion. J. Petrol. 20, 421–486.

Pham, M., Menzies, A. J., 1993. Results from a field-wide numerical model of the Geysers geothermal field, California. Geotherm. Resour. Council Transact. 17, 259–265.

Pruess, K., Oldenburg, C., Moridis, G., 1999. TOUGH2 User's Guide, Version 2.0. Report LBNL-43134, Lawrence Berkeley Nat. Lab, Berkeley, CA.

Schriener, Jr., A., Suemnicht, G. A., 1980. Subsurface intrusive rocks at The Geysers geothermal area, California. In: Silberman, M. C., *et al.* (eds.), Proceedings of Sympos. Miner. Depos. Pacific NW, U. S. Geol. Survey, Denver, CO, pp. 294–303, open File Rept. 81-355.

Stanley, W. D., Blakely, R. J., 1995. The Geysers-Clear Lake Geothermal Area, CA-An updated geophysical perspective of heat sources. Geothermics 24 (2), 187–221.

Thompson, R. C., 1992. Sturctural stratigraphy and intrusive rocks at The Geysers Geothermal field. Geotherm. Resour. Council Transact. 17, 59–63.

Truesdell, A. H., Kennedy, B. M., Walters, M. A., D'Amore, F., 1995. New evidence for a magmatic origin of some gases in The Geysers geothermal reservoir. In: Proc. 19th Workshop on Geothermal Reservoir Engineering, Stanford Univ., Stanford, CA, pp. 297–301.

Walters, M. A., Combs, J., 1992. Heat flow in The Geysers-Clear Lake geothermal area of Northern California, U.S.A. In: Stone, C. (ed.), Monograph on The Geysers geothermal field, Geothermal Resour. Council, Sacramento, CA, vol. 17 of *Special Report*, pp. 43–58.

Walters, M. A., Moore, J. N., Nash, G. D., Renner, J. L., 1996. Oxygen Isotope Systematics and Reservoir Evolution of the Northwest Geysers, CA. Geotherm. Resour. Council Transact. 20, 413–421.

Williamson, K. H., 1990. Reservoir simulation of The Geysers geothermal field. In: Proceedings, 15th Workshop on Geothermal Reservoir Engineering, Stanford Univ., Stanford, CA, vol. SGP-TR-130, pp. 113–123.

C Preprint: 2001 Stanford Geothermal Workshop Paper

MODELING SUPERCRITICAL SYSTEMS WITH TOUGH2: PRELIMINARY RESULTS USING THE *EOS1sc* EQUATION OF STATE MODULE

Tom Brikowski
Geosciences Dept., University of Texas at Dallas
Richardson, TX 75083 USA, email: brikowi@utdallas.edu

Abstract

Supercritical fluid conditions (T>374°C) have been observed at depth in magmatic geothermal systems and are important in the deep heating zones of extensional geothermal systems as well. As interest in the sustainability of mature geothermal fields increases, and as exploration for high temperature resources becomes more attractive, the ability to model an entire field from ground surface to supercritical regions will become crucial. A super-critical equation-of-state module (*EOS1sc*) is under development to extend the range of applicability of *TOUGH2* to such conditions, using a numerical equation of state for pure H_2O, This *EOS1sc* module successfully reproduces sub-critical sample problem results of EOS1 (e.g. RVF, RFP). Large gradients in fluid properties are typical in near-critical point conditions, and therefore convergent supercritical models using *EOS1sc* are currently limited to moderately convective scenarios. Model results for such a system, depicting geothermal production/injection (i.e. forced-convection) under supercritical conditions, based on the *TOUGH2* RFP sample problem, are provided to demonstrate the current capabilities of *EOS1sc*.

C.1 INTRODUCTION

Supercritical fluid conditions (T>374°C , Fig. 31) have been observed at depth in magmatic geothermal systems (Kakkonda, Japan; *Ikeuchi et al.*, 1998) and are implied in the deeper portions of extensional geothermal systems as well (Basin and Range, Nevada, USA; Wisian, 2000). As interest in the sustainability of mature geothermal fields increases, and as exploration for high temperature resources becomes more attractive (e.g. Iceland; Fridleifsson and Albertsson, 2000), the ability to model an entire field from ground surface to supercritical regions will become crucial. There are currently few options in selecting a supercritical geothermal reservoir modeling computer program. The most commonly-applied programs, *TOUGH2* (*Pruess et al.*, 1999) and *TETRAD* (*Vinsome*, 1990), are currently limited to sub-critical conditions. The most readily-available supercritical program (*HYDROTHERM*, *Hayba and Ingebritsen*, 1994) lacks some of the computational and gridding flexibility of *TOUGH2*. Given this situation, a super-critical equation-of-state (EOS) module for *TOUGH2* would be an attractive option; this paper is a report of progress on that task.

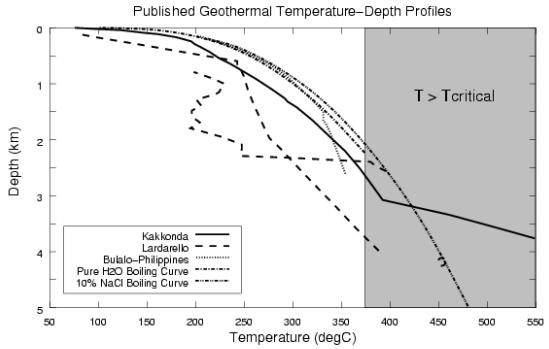

Figure 17: Pressure-depth profiles for deep geothermal systems, after *Muraoka et al.* (2000). Shaded area shows region of supercritical temperatures.

That super-critical EOS (*EOS1sc*) is based on the numerical equation of state for pure H_2O (*H2092*) developed by *Johnson and Norton* (1991), which in turn is based on the mathematical equations of state developed by Haar *et al.* (1984) and *Levelt-Sengers et al.* (1983). The latter equations provide extremely accurate thermodynamic properties in the critical region. Models of super-critical hydrothermal systems demonstrate strong attraction to near-critical conditions (*Brikowski*, 2001b; *Brikowski and Norton*, 1989; *Hayba and Ingebritsen*, 1997; *Norton and Knight*, 1977), and accurate modeling of these conditions is crucial for accurate modeling of such systems.

C.2 SUPERCRITICAL SIMULATORS

Readily available (primarily non-commercial) geothermal reservoir simulation computer programs exhibit a wide variety of capabilities. Selection of the optimal code for application to supercritical geothermal systems is problematic. For the most accurate models of such systems, a code must allow for two or more fluid phases, treat near-critical fluid properties extremely accurately, and ideally consider tracer transport (with water-rock interaction) to further constrain the thermal models. A variety of matrix solution options and flexible gridding (e.g. finite element) are a distinct advantage when modeling natural systems. It was determined that a modified version of *TOUGH2* would best meet these criteria, but a review of other options is warranted.

C.2.1 *HYDROTHERM*

Released in 1994, *HYDROTHERM* became the first widely-available geothermal reservoir simulator to include both two-phase and supercritical conditions (*Hayba and Ingebritsen*, 1994). This finite-difference code is based on the earlier *GEOTHER* (Faust and Mercer, 1979), and utilizes fluid enthalpy and pressure as its primary (dependent) variables. Fluid (pure H_2O) properties are calculated using smoothed bicubic interpolation of lookup tables based on steam table compilations by Haar *et al.* (1984), and an extended equation for fluid viscosities presented by Sengers and Kamgar-Parsi (1984). Solution of the non-linear finite difference equations is accomplished using slice-successive overrelaxation for matrix solution embedded in Newton-Raphson iteration for the non-linear parameters. An example of application of this code is a study of convection in hypothetical pluton settings (*Hayba and Ingebritsen*, 1997). Likely difficulties in implementing tracer transport and water-rock interaction modeling in a finite-difference formulation precluded the use of this code.

C.2.2 *TETRAD*

TETRAD is a versatile reservoir simulator primarily concerned with multiphase petroleum and geothermal settings (*Vinsome*, 1990). Fluid and rock matrix can be compressible. Fluid properties are computed using user-settable values or steam table, and allows for an essentially limitless pressure-temperature-salinity range. Treatment of critical-point phenomena (i.e. termination of the two-phase boundary) would be difficult with such a formulation. *TETRAD* allows for computation of dissolved species transport. The program is based on the finite difference method, with Newton-Raphson iteration and pre-conditioned iterative solution of the matrices. This program has been used for detailed studies of liquid adsorption (Shook, 1994). Probable limitations in treatment of near-critical phenomena made this code unlikely to be the best candidate for this study.

C.2.3 *MARIAH*

This finite element program was originally written at Sandia National Laboratory for modeling of single phase, incompressible fluid (pure H_2O) flow in sub-critical conditions (Gartling and Hickox, 1982). Since that time it has been extensively modified by this author to treat supercritical (single-phase) conditions (Brikowski and Norton, 1986) using *H2092*. This routine provides continuous, very accurate fluid properties over the range 0-1200 °C and 0-3000 MPa, with particular accuracy near the critical point. Although computationally intensive, this continuity has proven crucial in obtaining numerical solutions for systems that bracket the critical point of H_2O.

In recent years, *MARIAH* has been modified to include modeling of water-rock interaction and transport of oxygen isotopes (i.e. ^{18}O, Brikowski, 1995), with subsequent application to natural state models of The Geysers (*Brikowski*, 2001b; Brikowski, 2000; Brikowski and Norton, 1999). These models demonstrate the importance of near-critical phenomena in controlling the nature of high-temperature geothermal/hydrothermal systems, and the utility of $\delta^{18}O$-alteration as a tight constraint on models of such systems. While the flexible gridding allowed by the finite-element formulation of *MARIAH* is highly advantageous, the prospect of conversion of this code to treat two-phase compressible fluids was daunting.

C.2.4 *H2092*

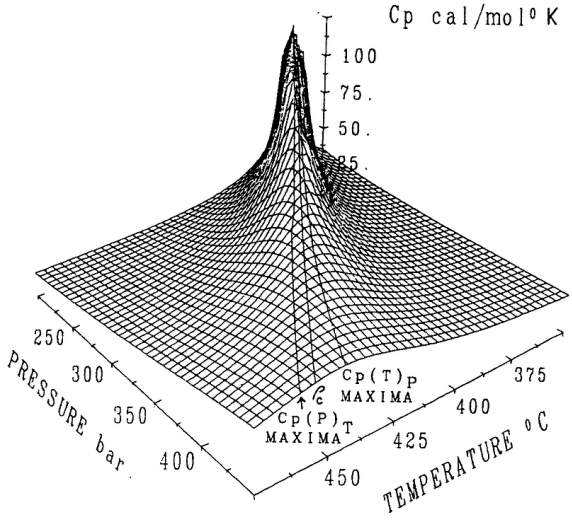

Figure 18: Variation of isobaric heat capacity (C_p) for pure H_2O in the near super-critical region. Looking from high P and T down the critical isochore toward the critical point. C_p reaches infinite value at that point, surface has been truncated for graphical purposes. After *Johnson and Norton* (1991).

Although not a reservoir simulation code, *H2092* merits separate discussion. Fluid prop-

erties reach extrema at the critical point (e.g. isobaric heat capacity theoretically reaches $+\infty$, Fig. 18). These extrema have a profound effect on fluid dynamics, and accurate treatment of such properties is required for accurate reservoir models that include the critical region. *H2092* uses a Taylor series approximation for Helmholtz free energy outside the critical region, from which most of the remaining fluid thermodynamic properties can be obtained via numerical differentiation (pg. 580, *Johnson and Norton*, 1991). In the vicinity of the critical point, the alternative Levelt-Sengers equation for thermodynamic potential, which can be treated similarly to obtain fluid properties. Given input T-P or T-ρ, *H2092* computes a total of eighteen fluid thermodynamic properties and ratios. The Taylor series are based on physical considerations of the internal chemistry of the fluid, and as such will be far more accurate than strictly mathematical interpolations of these properties (e.g. *International Formulation Committee*, 1967). For systems containing critical-point conditions this accuracy is fundamentally important, but it comes at a steep computational cost, since the Taylor series require calculation of many more terms at each P-T point. The code is freely available as a part of the SUPCRT aqueous geochemical modeling package (Johnson *et al.*, 1992).

C.2.5 *TOUGH2*

This program is a refinement of the MULKOM code system developed over several decades at Lawrence Berkeley National Laboratory. The program employs the integrated finite difference method, allowing for flexible gridding, treats multi-phase subcritical fluid and heat flow, using Newton-Raphson iteration and a user-selectable variety of matrix solution techniques. It has been qualified for use as the unsaturated zone performance assessment code for the Yucca Mountain Nuclear Waste Repository. The flexibility of this program, particularly in terms of two-phase phenomena and matrix solution approaches make it an attractive candidate for supercritical modeling. An extensive bibliography of literature on *TOUGH2* and its applications is available on the Internet at http://ccs.lbl.gov/TOUGH2/BIBLIOGRAPHY.html.

C.3 APPROACH

Since no one of the codes described above is capable of modeling supercritical conditions with the desired level of detail, as well as modeling dissolved species transport and water-rock interaction, some hybrid of the codes will be required. The apparent optimal choice for this hybrid is *TOUGH2*, modified to include first a supercritical equation of state (*H2092*), and later the oxygen-isotope alteration routines from *MARIAH*. The subject of this paper are the results of the first coding phase of the project, in which *H2092* will be adapted as an EOS module, to serve as a plug-in conversion to enable supercritical modeling. The supercritical equation of state module has been designated as "*EOS1sc*", and its structure largely imitates that of the original EOS1 module avaliable with *TOUGH2* (*Pruess et al.*, 1999). The implementation of *EOS1sc* extends the range of *TOUGH2* considerably, currently giving it an applicable range of $0 < T \leq 1000$°C and $0 < P \leq 1000$ MPa (Fig. 33)

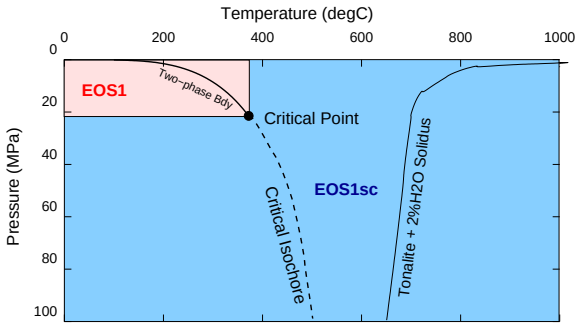

Figure 19: P-T Validity Range of eos1 (pink shaded area, *Pruess et al.*, 1999) and *EOS1sc* (blue area). Liquid-vapor solidus of hydrous tonalite magma with 2 wt% H_2O shown to indicate typical magmatic conditions (*Whitney*, 1975). Dashed line shows approximate location of critical isochore (line of density equal to density at the critical point).

C.3.1 Challenges

A number of conceptual and numerical challenges in this approach were predictable, and were encountered. Most problematic is the termination of the two-phase boundary at the critical point. All of the reservoir simulators listed above utilize phase mass-balances which are computed at every point in the system. Both steam and liquid "disappear" above the critical point, and become an indistinguishable supercritical fluid. At and above the critical point, this requires an artificial iso-enthalpic "reaction" (e.g. *Hayba and Ingebritsen*, 1994, p. 8) to convert steam or liquid into fluid. *HYDROTHERM* handles this problem by declaring 50% saturation with identical steam and liquid properties in supercritical regions. Since *TOUGH2* utilizes steam saturation as a primary (dependent) variable along the two-phase boundary, this approach was not an option. Instead an artificial extension to the two-phase boundary was implemented, across which a thermodynamically-neutral reaction of liquid and steam was allowed. Although many orientations for this extension are possible, extending it along the critical isochore (line of density equal to that at the critical point, dashed line, Fig. 33) was conceptually the simplest. A more difficult problem is implied phase transitions (a super-critical cell with sub-critical neighbor). These lead to "subtle and complicated difficulties" (e.g. *Pruess et al.*, 1999, Appendix D) or (e.g. *Hayba and Ingebritsen*, 1994, p. 8) in computing accurate phase mass balances, and care must be taken to treat interfacial fluxes properly. Variable switching in *TOUGH2* to pressure-saturation along the two-phase boundary becomes somewhat problematic at the critical point. Finally, a problem that will never be completely eliminated is difficult convergence near the critical point. The incorporation of *H2092* is specifically intended to treat extrema in fluid properties accurately, based on the proposition that these extrema are the fundamental controls on fluid circulation and heat transport in deep systems. As a result spatial gradients in fluid properties are larger than with alternative equations of state described above. This leads to increased residuals (errors) in mass and energy balance equations, and increased difficulty in finding convergent solutions for problems with coarse grid and high advective flow rates. At the time of this writing, *EOS1sc* succeeds only in forced-convection problems, where

non-linear effects on flow rates are minimized. This restriction will hopefully be resolved in the future.

C.4 RESULTS

Tests of *EOS1sc* have been made in two categories. The first are sub-critical models run to confirm that existing capabilities of *TOUGH2* have not been degraded by the application of *EOS1sc*. The second explore the supercritical performance of *EOS1sc*, and are more limited, since successful supercritical runs have only recently been achieved.

C.4.1 Sub-Critical Tests

For general familiarity, the two sample problems distributed with *TOUGH2* that invoke the EOS1 module were run for comparison. These are RFP, the "geothermal five-spot injection/production" problem (sec. 9.4, *Pruess et al.*, 1999), and RVF, the "heat sweep in a vertical fracture" problem. Both runs produce results that are graphically indistinguishable from the EOS1 results (Figs. 26 and 27. In detail, results differ by less than 0.01%, running in double-precision (REAL*8). As expected, a significant difference in run-times is apparent (Fig. 28), with the *EOS1sc* runs requiring 5 to 50 times longer on an SGI O2 R10000 workstation. Since memory usage is small, and disk access minimal in these test problems, similar time differences should be experienced on most computing platforms. Recall that EOS1 has been optimized for speed in sub-critical settings, while *EOS1sc* has been constructed for maximum accuracy in the near-critical region. Users wishing to apply *EOS1sc* should be thoroughly committed to thermodynamic accuracy versus computational speed.

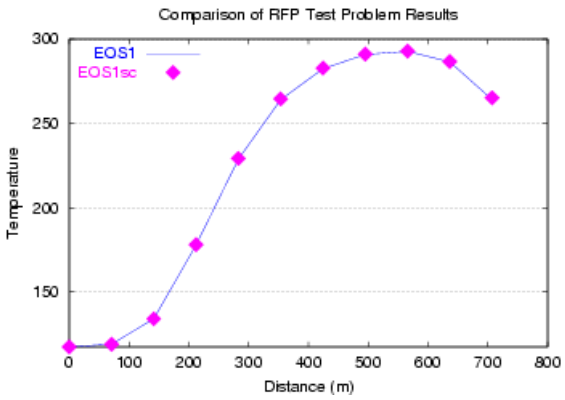

Figure 20: RFP (geothermal 5-spot well) test results for EOS1 (line) and *EOS1sc* (points) in *TOUGH2*. See *Pruess et al.* (sec. 9.4, 1999) for details of problem specification.

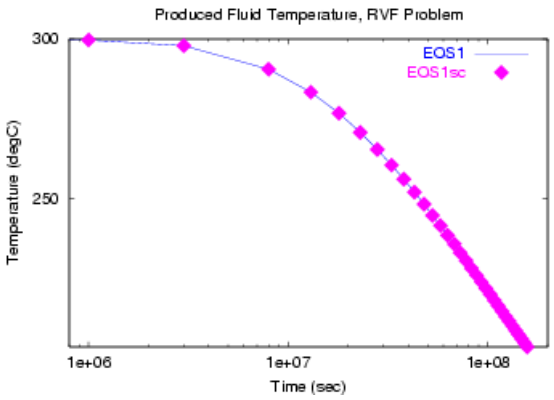

Figure 21: RVF (vertical fracture heat-sweep) test results using EOS1 (line) and *EOS1sc* (points) in *TOUGH2*. See *Pruess et al.* (sec. 9.3, 1999) for details of problem specification.

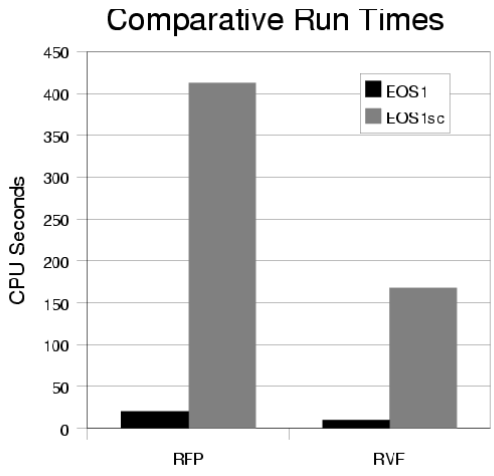

Figure 22: Comparative run times, EOS1 (blue) and *EOS1sc* (magenta). *EOS1sc* runs require 5-10 times more CPU time, since series-based computation of water properties is extremely accurate but time-consuming.

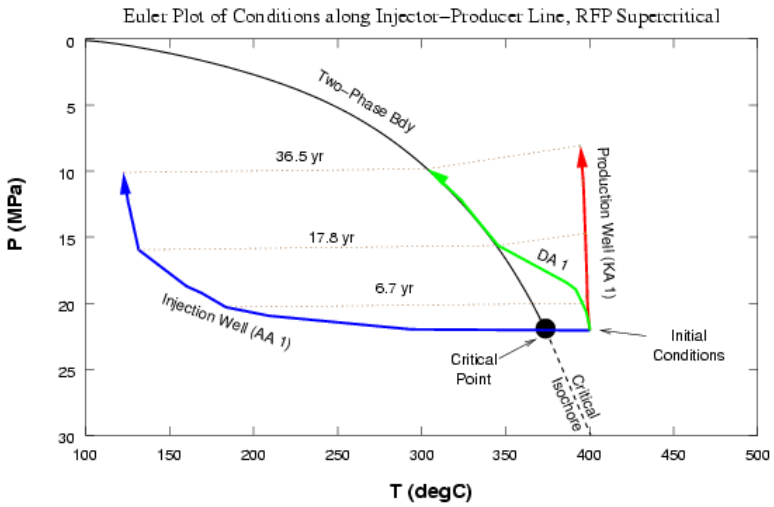

Figure 23: Supercritical RFP test results using *EOS1sc*. Variation of P-T conditions with time at three points along injector-producer line. Points at representative times connected by dashed lines. Injector point migrates rapidly from supercritical initial conditions through critical point to cool liquid conditions. Intermediate point "DA 1" follows boiling curve, production point show isothermal depressurization.

C.4.2 Supercritical Tests

For familiarity, RFP, the sub-critical EOS1 sample problem treating the "five-spot" injection/production geometry was extended to supercritical conditions. Starting conditions in the reservoir were specified similar to those found at the bottom of well WD-1a at Kakkonda, Japan (*Ikeuchi et al.*, 1998), albeit ignoring the very high salinities encountered at those depths. This test is meant to simulate the conditions that might be encountered in production from a barely supercritical reservoir, e.g. as proposed by Fridleifsson and Albertsson (2000) and modeled by Yano and Ishido (1998). Problem specifications are identical to the RFP problem included in the *TOUGH2* distribution, except that rock initial temperature is set to 400°C , pressure at 22.06 MPa (critical point is located at 373.917 °C , 22.046 MPa, *Levelt-Sengers et al.*, 1983). Fluids at 100 °C are injected at the center of the 5-spot grid, and are withdrawn at an identical rate at the corner of the grid. Non-convergence (using the solver settings given in the distributed RFP file) forced reduction of the pumping rate from 3 kg/sec steam in the subcritical case, to 0.9 kg/sec. Grid refinement was not attempted, but would presumably allow convergence for the higher pumping rate. P-T conditions in the reservoir sweep across the critical point, with the injection point moving rapidly to lower temperatures, then all points moving more slowly upward to lower pressures (Fig. 29). Intermediate points (e.g. element "DA 1", blue line, Fig. 29) quickly migrate to the two-phase boundary, and proceed along it until the end of the simulation. Since the P-T profile between injector and producer (dashed lines, Fig. 29) migrate across the critical point, implied phase transitions are encountered in the grid and are successfully treated by *EOS1sc*.

C.5 SUMMARY

A supercritical equation of state for pure H_2O has been developed for use with *TOUGH2*. This module extends the range of *TOUGH2* to beyond typical silicic magma solidus conditions, thereby allowing the modeling the entirety of magmatic and other high-temperature geothermal systems. Deep exploration and concerns about sustainable management of geothermal resources require that these deep roots of the system be considered. Preliminary testing of the module indicates that it preserves existing accuracy of *TOUGH2* at subcritical conditions, and successfully extends the modeling capabilities to supercritical conditions. Most problematic are systems that contain the critical point, e.g. any system with atmospheric conditions at the top, and supercritical conditions at depth. Difficult solution convergence owing to accurate treatment of fluid property extrema near the critical point currently limits the capability of *TOUGH2* with *EOS1sc* to settings that involve forced convection, or limited fluid velocities. Ongoing testing and software modification is addressing these issues.

C.6 ACKNOWLEDGMENTS

This research supported by U. S. Dept. of Energy grant DE-FG07-98ID13677 to UTD, with subcontracts to David Blackwell of SMU and Denis Norton, consultant, Stanley ID. Their contributions to the conceptual aspects of this software development have been crucial. James Johnson of LLNL provided the source code for *H2092*. Karsten Pruess provided encouragement in the early stages of this development. Invaluable periodic testing of earlier versions of *EOS1sc* has been carried out by Ken Wisian of SMU.

References

Brikowski, T. H., 1995. Isotope-calibrated hydrothermal models: Geothermal implications of a model of the Skaergaard Intrusion. Geotherm. Resour. Council Transact. 19, 171–176.

Brikowski, T. H., 2000. Using isotopic alteration modeling to explore the Natural State of The Geysers geothermal system, USA. In: Proceedings of the World Geothermal Congress, pp. 2045–50, kyushu-Tohoku, Japan.

Brikowski, T. H., 2001. Deep fluid circulation and isotopic alteration in The Geysers geothermal system: Profile models. Geothermics 30 (2-3), 333–47, URL http://www.utdallas.edu/~brikowi/Research/Geysers/Geothermics2K/.

Brikowski, T. H., Norton, D., 1986. Consequences of magma chamber geometry on the thermal history of mid-ocean ridges. EOS 67, 1021.

Brikowski, T. H., Norton, D., 1989. Influence of magma chamber geometry on hydrothermal activity at mid-ocean ridges. Earth Planet. Sci. Lett. 93, 241–255.

Brikowski, T. H., Norton, D., 1999. An isotope-calibrated natural state model of The Geysers geothermal system: Initial results. Geotherm. Resour. Council Transact. 23, 347–350.

Faust, C. R., Mercer, J. W., 1979. Geothermal reservoir simulation: 1. Mathematical models for liquid- and vapor-dominated hydrothermal systems. Water Resour. Res. 15, 23–46.

Fridleifsson, G. O., Albertsson, A., 2000. Deep geothermal drilling on the Reykjanes Ridge: Opportunity for international collaboration. In: Proceedings of the World Geothermal Congress 2000, International Geothermal Organization, pp. F7–5, paper R0882.

Gartling, D. K., Hickox, C. E., 1982. MARIAH-A finite element computer program for incompressible porous flow problems : User's Manual. Tech. rep., Sandia National Labs.

Haar, L., Gallagher, J. G., Kell, G. S., 1984. NBS/NRC Steam Tables. Hemisphere Publishers, Washington, D.C.

Hayba, D. O., Ingebritsen, S. E., 1994. The computer model HYDROTHERM, a three-dimensional finite-difference model to simulate ground-water flow and heat transport in the temperature range of 0 to 1,200 degrees C. Wri 94-4045, U. S. Geol. Survey, Denver, CO.

Hayba, D. O., Ingebritsen, S. E., 1997. Multiphase groundwater flow near cooling plutons. J. Geophys. Res. 102 (6), 12235–12252.

Ikeuchi, K., Doi, N., Skagawa, Y., Kamenosono, H., Uchida, T., 1998. High-temperature measurements in well WD-1a and the thermal structure of the Kakkonda geothermal system, Japan. Geothermics 27 (5/6), 591–607.

International Formulation Committee, 1967. A formulation of the thermodynamic properties of ordinary water substance. IFC Secretariat, Düsseldorf, Germany.

Johnson, J. W., Norton, D., 1991. Critical phenomena in hydrothermal systems: State thermodynamic, electrostatic, and transport properties of H_2O in the critical region. Am. J. Sci. 291, 541–648.

Johnson, J. W., Oelkers, E. H., Helgeson, H. C., 1992. SUPCRT92; a software package for calculating the standard molal thermodynamic properties of minerals, gases, aqueous species, and reactions from 1 to 5000 bar and to 1000 degrees C. Computers & Geosciences 18 (7), 899–947.

Levelt-Sengers, J. M. H., Kamgar-Parsi, B., Balfour, F. W., Sengers, J. V., 1983. Thermodynamic properties of steam in the critical region. J. Phys. Chem. Ref. Data 5 (1), 1–51.

Muraoka, H., Yasukawa, K., Kimbara, K., 2000. Current state of development of deep geothermal resources in the world and implications to the future. In: Iglesias, E., Blackwell, D., Hunt, T., Lund, J., Tmanyu, S. (eds.), Proceedings of the World Geothermal Congress 2000, International Geothermal Association, pp. 1479–1484.

Norton, D., Knight, J., 1977. Transport phenomena in hydrothermal systems: Cooling plutons. Am. J. Sci. 277, 937–981.

Pruess, K., Oldenburg, C., Moridis, G., 1999. TOUGH2 User's Guide, Version 2.0. Report LBNL-43134, Lawrence Berkeley Nat. Lab, Berkeley, CA.

Sengers, J. V. L., Kamgar-Parsi, B., 1984. Representative equations for the viscosity of water substance. J. Physical and Chemical Reference Data 13, 185–205.

Shook, G. M., 1994. Effects of adsorption on exploitation of geothermal reservoirs. Geotherm. Resour. Council Transact. 18, 339–346.

Vinsome, K., 1990. TETRAD User Manual. Dyad Engineering,, Calgary, Alberta, Canada.

Whitney, J. A., 1975. The effects of pressure, temperature and χ_{H_2O} on phase assemblage in four synthetic rock compositions. J. Geol. 83, 1–31.

Wisian, K. W., 2000. Insights into Extensional Geothermal Systems from Numerical Modeling. Geotherm. Resour. Council Transact. 24, 281–286.

Yano, Y., Ishido, T., 1998. Numerical Investigation of Production Behavior of Deep Geothermal Reservoirs at Super-Critical Conditions. Geothermics 27 (5/6), 705–721.

D Preprint: 2001 GRC Paper

Modeling Supercritical Systems With Tough2: The *EOS1sc* Equation of State Module and a Basin and Range Example

Tom H. Brikowski

Geosciences Dept., University of Texas at Dallas, Richardson, TX 75083 USA, email: brikowi@utdallas.edu

Keywords: reservoir model, supercritical fluid, equation of state, reservoir simulator, software

Abstract

A supercritical fluid equation of state module (*EOS1sc*) has been developed for use with the *TOUGH2* geothermal reservoir simulator. Supercritical fluid conditions (T>374°C) have been observed at depth in magmatic geothermal systems and are important in the deep heating zones of extensional geothermal systems as well. As interest in the sustainability of mature geothermal fields increases, and as exploration for high temperature resources becomes more attractive, the ability to model an entire field from ground surface to supercritical regions will become crucial. Tests using the *EOS1sc* module successfully reproduce sub-critical sample problem results of EOS1. Supercritical validation suites are currently lacking, but preliminary models reasonably extend sub-critical model results to supercritical conditions. For example, generic models of extensional settings using *EOS1sc* with supercritical temperatures at depth better-simulate observed temperature depth profiles (e.g. Dixie Valley, NV) than EOS1-based models.

D.1 Introduction

Supercritical fluid conditions (T>374°C , Fig. 31) have been observed at depth in magmatic geothermal systems (Kakkonda, Japan; *Ikeuchi et al.*, 1998) and are implied in the deeper portions of extensional geothermal systems as well (Basin and Range, Nevada, USA; Wisian, 2000). As interest in the sustainability of mature geothermal fields increases, and as exploration for high temperature resources becomes more attractive (e.g. Iceland, Fridleifsson and Albertsson, 2000), the ability to model an entire field from ground surface to supercritical regions will become crucial. There are currently few options in selecting a supercritical geothermal reservoir modeling computer program. The most commonly-applied programs, *TOUGH2* (*Pruess et al.*, 1999) and *TETRAD* (*Vinsome*, 1990), are currently limited to sub-critical conditions (white area, Fig. 31). The most readily-available supercritical pro-

gram (*HYDROTHERM*, *Hayba and Ingebritsen*, 1994) lacks some of the computational and gridding flexibility of *TOUGH2*. Given this situation, a super-critical equation-of-state (EOS) module for *TOUGH2* would be an attractive option; this paper introduces such a module, and demonstrates its current applicability.

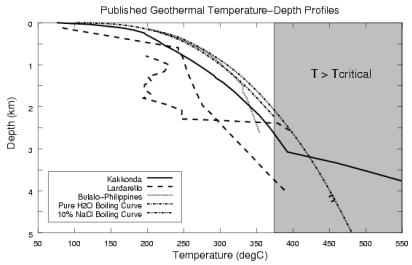

Figure 24: Pressure-depth profiles for deep geothermal systems, after *Muraoka et al.* (2000). Shaded area shows region of supercritical temperatures.

D.2 Approach

Since no one of the codes listed above is capable of modeling supercritical conditions with the desired level of thermodynamic detail, as well as modeling dissolved species transport and water-rock interaction, some modification of the codes will be required. The apparent optimal choice for this hybrid is *TOUGH2*, modified to include first a supercritical equation of state (*H2092*), and later the oxygen-isotope alteration routines from *MARIAH*. The subject of this paper are the results of the first coding phase of the project, in which *H2092* will be adapted as an EOS module, to serve as a plug-in conversion to allow supercritical modeling. The supercritical equation of state module has been designated as "*EOS1sc*", and its structure largely imitates that of the original EOS1 module avaliable with *TOUGH2* (*Pruess et al.*, 1999). The implementation of *EOS1sc* extends the range of *TOUGH2* considerably, currently giving it an applicable range of $0 < T \leq 1000$°C and $0 < P \leq 1000$ MPa (Fig. 33)

D.2.1 Supercritical Equation of State (*H2092*)

The numerical equation of state used in this modification, *H2092*, has been used in a number of previous supercritical applications (*Brikowski and Norton*, 1989; *Norton and Hulen*, 2001). It treats very accurately fluid properties and their extrema at the critical point (e.g. isobaric heat capacity theoretically reaches $+\infty$). These extrema have a profound effect on fluid dynamics, and accurate treatment of such properties is required for accurate reservoir models that include the critical region. *H2092* uses a Taylor series approximation for Helmholtz free

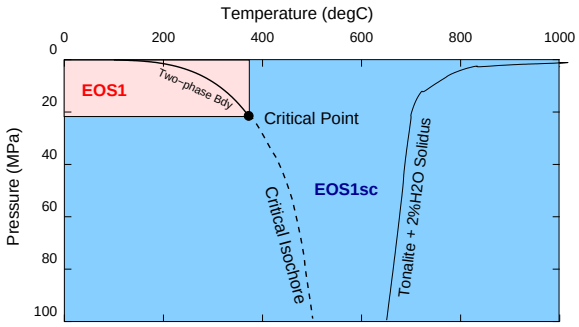

Figure 25: P-T Validity Range of EOS1 (white area, *Pruess et al.*, 1999) and *EOS1sc* (grey area). Liquid-vapor solidus of hydrous tonalite magma with 2 wt% H_2O shown to indicate typical magmatic conditions (*Whitney*, 1975). Dashed line shows approximate location of critical isochore (line of density equal to density at the critical point).

energy outside the critical region, from which most of the remaining fluid thermodynamic properties can be obtained via numerical differentiation (*Johnson and Norton*, 1991, pg. 580). In the vicinity of the critical point, the non-classical Levelt-Sengers equation for thermodynamic potential is used, which can be treated similarly to obtain fluid properties. Given input T-P or T-ρ, *H2092* computes a total of eighteen fluid thermodynamic properties and ratios. The Taylor series are based on physical considerations of the internal chemistry of the fluid, and as such can be far more accurate than strictly mathematical interpolations of these properties (e.g. *International Formulation Committee*, 1967). For systems containing critical-point conditions this accuracy is fundamentally important, but it comes at a steep computational cost, since the Taylor series require calculation of many more terms at each P-T point. The *H2092* code is freely available as a part of the SUPCRT aqueous geochemical modeling package (Johnson *et al.*, 1992).

D.2.2 Challenges

A number of conceptual and numerical challenges in this approach were predictable, and were encountered. Most problematic is the termination of the two-phase boundary at the critical point. All of the reservoir simulators listed above utilize phase mass-balances which are computed at every point in the system. Both steam and liquid "disappear" above the critical point, and become an indistinguishable supercritical fluid. At and above the critical point, this requires an artificial iso-enthalpic "reaction" (e.g. *Hayba and Ingebritsen*, 1994, p. 8) to convert steam or liquid into a supercritical fluid. *HYDROTHERM* handles this problem by declaring 50% saturation with identical steam and liquid properties in supercritical regions. Since *TOUGH2* utilizes steam saturation as a primary (dependent) variable along the two-phase boundary, this approach was not an option. Instead an artificial extension to the two-phase boundary was implemented, across which a thermodynamically-neutral reaction of liquid and steam was allowed. Although many orientations for this extension are possible, placing it along the critical isochore (line of density equal to that at the critical point; dashed

line, Fig. 33) was conceptually the simplest.

A more difficult problem is implied phase transitions (a super-critical cell with sub-critical neighbor). These lead to "subtle and complicated difficulties" (e.g. *Pruess et al.*, 1999, Appendix D) or (e.g. *Hayba and Ingebritsen*, 1994, p. 8) in computing accurate phase mass balances, and care must be taken to treat interfacial fluxes properly. Variable switching in *TOUGH2* to pressure-saturation along the two-phase boundary becomes somewhat problematic at the critical point. Finally, a problem that will never be completely eliminated is difficult convergence near the critical point. The incorporation of *H2092* is specifically intended to treat extrema in fluid properties accurately, based on the proposition that these extrema are the fundamental controls on fluid circulation and heat transport in deep systems. As a result spatial gradients in fluid properties are larger than with alternative equations of state described above. This leads to increased residuals (errors) in mass and energy balance equations, and increased difficulty in finding convergent solutions for problems with coarse grid and high advective flow rates. Unsmoothed initial conditions can also be problematic.

D.3 Results

Tests of *EOS1sc* have been made in two categories. The first are sub-critical models run to confirm that existing capabilities of *TOUGH2* have not been degraded by the application of *EOS1sc*. The second explore the supercritical performance of *EOS1sc*, and are more limited, since successful supercritical runs have only recently been achieved.

D.3.1 Sub-Critical Tests

For general familiarity, the two sample problems distributed with *TOUGH2* that invoke the EOS1 module were run for comparison. These are RFP, the "geothermal five-spot injection/production" problem (*Pruess et al.*, 1999, sec. 9.4), and RVF, the "heat sweep in a vertical fracture" problem. Both runs produce results that are graphically indistinguishable from the EOS1 results (Figs. 26 and 27). In detail, results differ by less than 0.01%, running in double-precision (REAL*8). As expected, a significant difference in run-times is apparent (Fig. 28), with the *EOS1sc* runs requiring 5 to 50 times longer on an SGI O2 R10000 workstation. Since memory usage is small, and disk access minimal in these test problems, similar time differences should be experienced on most computing platforms. Recall that EOS1 has been optimized for speed in sub-critical settings, while *EOS1sc* has been constructed for maximum accuracy in the near-critical region. Users wishing to apply *EOS1sc* should be thoroughly committed to thermodynamic accuracy versus computational speed.

D.3.2 Supercritical Tests

Geothermal Five-Spot (RFP) For familiarity, RFP, the sub-critical EOS1 sample problem treating the "five-spot" injection/production geometry was extended to supercritical con-

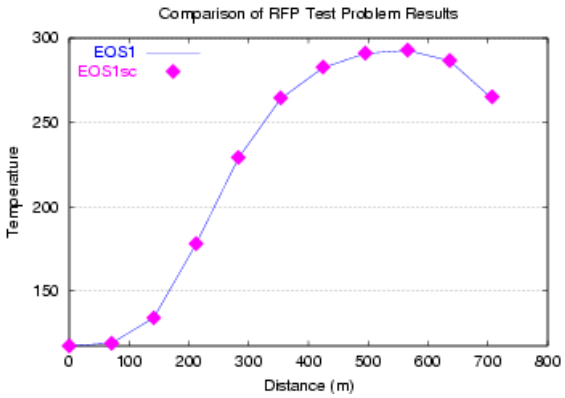

Figure 26: RFP (geothermal 5-spot well) test results for EOS1 (line) and *EOS1sc* (points) in *TOUGH2*. See *Pruess et al.* (1999, sec. 9.4) for details of problem specification.

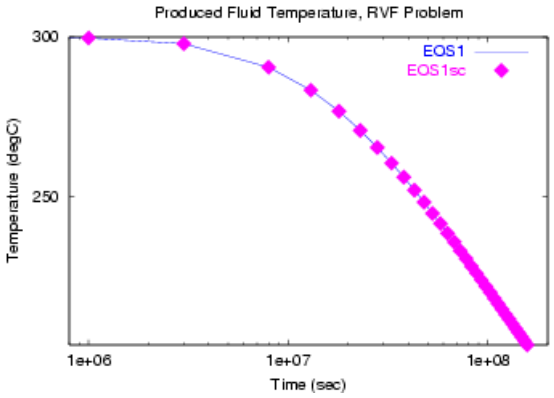

Figure 27: RVF (vertical fracture heat-sweep) test results using EOS1 (line) and *EOS1sc* (points) in *TOUGH2*. See *Pruess et al.* (1999, sec. 9.3) for details of problem specification.

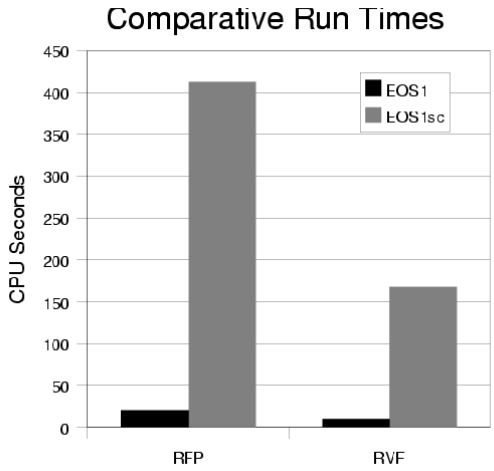

Figure 28: Comparative run times, EOS1 (black) and *EOS1sc* (gray). *EOS1sc* runs require 5-10 times more CPU time, since series-based computation of water properties is extremely accurate but time-consuming.

ditions. Starting conditions in the reservoir were specified similar to those found at the bottom of well WD-1a at Kakkonda, Japan (*Ikeuchi et al.*, 1998), albeit ignoring the very high salinities encountered at those depths. This test is meant to simulate the conditions that might be encountered in production from a barely supercritical reservoir, e.g. as proposed by Fridleifsson and Albertsson (2000) and modeled by Yano and Ishido (1998). Problem specifications are identical to the RFP problem included in the *TOUGH2* distribution, except that rock initial temperature is set to 400°C , pressure at 22.06 MPa (critical point is located at 373.917 °C , 22.046 MPa, *Levelt-Sengers et al.*, 1983). Fluids at 100 °C are injected at the center of the 5-spot grid, and are withdrawn at an identical rate at the corner of the grid. Non-convergence (using the solver settings given in the distributed RFP file) forced reduction of the production rate from 3 kg/sec steam in the subcritical case, to 0.9 kg/sec. Grid refinement was not attempted, but would presumably allow convergence for the higher pumping rate. P-T conditions in the reservoir sweep across the critical point, with conditions at the point of injection (element AA1) moving rapidly to lower temperatures, then all points moving more slowly upward to lower pressures (Fig. 29). Intermediate points (e.g. element "DA 1", Fig. 29) passes through the critical point of pure H_2O, and parallels the two-phase boundary after that. Since the P-T profile between injector and producer (dotted lines, Fig. 29) migrate across the critical point, implied phase transitions are encountered in the grid and are successfully treated by *EOS1sc*.

Generic Extensional Setting A number of detailed thermal models have been made of hypothetical (e.g. Forster and Smith, 1989; Wisian, 2000) and natural (e.g. Becker and Blackwell, 1993) extensional systems, primarily using the U.S. Basin and Range province as the basis for the models. In particular, Wisian (2000) models a hypothetical system similar to the

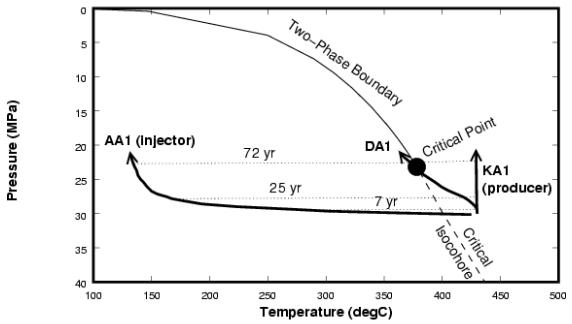

Figure 29: P-T paths for selected wells, supercritical RFP test using *EOS1sc*. Variation of P-T conditions with time at three points along the injector-producer line. Points at representative times connected by dashed lines. Injector point migrates rapidly from supercritical initial conditions through critical point to cool liquid conditions. Intermediate point "DA 1" passes directly through critical point, production point "KA1" shows isothermal depressurization.

geothermal system at Dixie Valley, NV. Comparison of temperature-depth profiles made with some of his models (using *TOUGH2* with EOS1, dotted line, Fig. 30) shows that modeled temperatures are well below those observed in deep wells in these systems. Wisian's models extend to 8 km depth in order to avoid boundary effects on fluid flow. At those depths in high heat-flow areas, conditions approach the critical point. To correctly model mass and heat balances in these systems, models must include super-critical conditions even though the produced fluids in such systems never experience such extreme temperatures. A simple experiment with increased (probably excessive) heat input at the base of such a model demonstrates that inclusion of supercritical conditions in the model (using *EOS1sc*, dashed line, Fig. 30) greatly improves the fit to observed temperature-depth profiles.

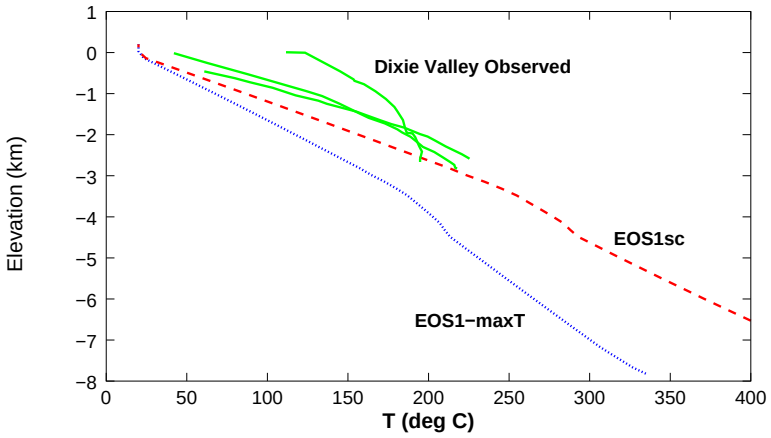

Figure 30: Basin and Range Model results compared to Dixie Valley observed T vs Z. Dotted line shows *TOUGH2* model results for generic extensional setting using EOS1 at maximum temperatures allowed by code (i.e. subcritical). Dashed line shows results using *EOS1sc* with supercritical conditions at depth. Solid lines show observed temperatures at Dixie Valley, NV (after Blackwell *et al.*, 2000). Incorporation of supercritical conditions appears to be necessary at base of these basin-scale models in order to match observed T-depth profiles. See Wisian (2000) for details of model construction.

D.4 Summary

A supercritical equation of state for pure H_2O has been developed for use with *TOUGH2*. This module extends the range of *TOUGH2* to beyond typical silicic magma solidus conditions, thereby allowing models of the entirety of magmatic and other high temperature geothermal systems. This allows the modeler to start from relatively reliable estimates of total mass or energy in the system, rather than having to impose arbitrary boundary conditions based on the limitations of the reservoir simulator. Deep exploration and concerns about sustainable management of geothermal resources require that these deep roots of the system be considered. Preliminary testing of the module demonstrates that it preserves existing accuracy of *TOUGH2* at subcritical conditions, and successfully extends the modeling capabilities to supercritical conditions. Most problematic are systems that contain the

critical point, e.g. any system with atmospheric conditions at the top, and supercritical conditions at depth. Difficult solution convergence owing to accurate treatment of fluid property extrema near the critical point requires careful application of *TOUGH2* with *EOS1sc*. Wise choice of matrix solvers, and minimization of steep pressure and temperature gradients in initial conditions generally overcomes these limitations.

D.5 Acknowledgments

This research supported by U. S. Dept. of Energy grant DE-FG07-98ID13677 to UTD, with subcontracts to David Blackwell of SMU and Denis Norton, consultant, Stanley ID. Their contributions to the conceptual aspects of this software development have been crucial. James Johnson of LLNL provided the source code for *H2092*. Karsten Pruess provided encouragement in the early stages of this development. Invaluable testing of earlier versions of *EOS1sc* has been carried out by Ken Wisian of SMU.

References

Becker, D. J., Blackwell, D., 1993. Gravity and hydrothermal modeling of the Roosevelt Hot Springs area, Southwestern Utah. J. Geophys. Res. 98, 17787–17800.

Blackwell, D. D., Golan, B., Benoit, D., 2000. Temperatures in the Dixie Valley, Nevada Geothermal System. Geotherm. Resour. Council Transact. 24, 223–28.

Brikowski, T. H., Norton, D., 1989. Influence of magma chamber geometry on hydrothermal activity at mid-ocean ridges. Earth Planet. Sci. Lett. 93, 241–255.

Forster, C., Smith, L., 1989. The influence of groundwater flow on thermal regimes in mountainous terrain: A model study. J. Geophys. Res. 94, 9439–9451.

Fridleifsson, G. O., Albertsson, A., 2000. Deep geothermal drilling on the Reykjanes Ridge: Opportunity for international collaboration. In: Proceedings of the World Geothermal Congress 2000, International Geothermal Organization, pp. F7–5, paper R0882.

Hayba, D. O., Ingebritsen, S. E., 1994. The computer model HYDROTHERM, a three-dimensional finite-difference model to simulate ground-water flow and heat transport in the temperature range of 0 to 1,200 degrees C. Wri 94-4045, U. S. Geol. Survey, Denver, CO.

Ikeuchi, K., Doi, N., Skagawa, Y., Kamenosono, H., Uchida, T., 1998. High-temperature measurements in well WD-1a and the thermal structure of the Kakkonda geothermal system, Japan. Geothermics 27 (5/6), 591–607.

International Formulation Committee, 1967. A formulation of the thermodynamic properties of ordinary water substance. IFC Secretariat, Düsseldorf, Germany.

Johnson, J. W., Norton, D., 1991. Critical phenomena in hydrothermal systems: State thermodynamic, electrostatic, and transport properties of H_2O in the critical region. Am. J. Sci. 291, 541–648.

Johnson, J. W., Oelkers, E. H., Helgeson, H. C., 1992. SUPCRT92; a software package for calculating the standard molal thermodynamic properties of minerals, gases, aqueous

species, and reactions from 1 to 5000 bar and to 1000 degrees C. Computers & Geosciences 18 (7), 899–947.

Levelt-Sengers, J. M. H., Kamgar-Parsi, B., Balfour, F. W., Sengers, J. V., 1983. Thermodynamic properties of steam in the critical region. J. Phys. Chem. Ref. Data 5 (1), 1–51.

Muraoka, H., Yasukawa, K., Kimbara, K., 2000. Current state of development of deep geothermal resources in the world and implications to the future. In: Iglesias, E., Blackwell, D., Hunt, T., Lund, J., Tmanyu, S. (eds.), Proceedings of the World Geothermal Congress 2000, International Geothermal Association, pp. 1479–1484.

Norton, D. L., Hulen, J. B., 2001. Geologic Analysis and Thermal-History Modeling of The Geysers Magmatic-Hydrothermal System. Geothermics 30 (2-3), 211–234.

Pruess, K., Oldenburg, C., Moridis, G., 1999. TOUGH2 User's Guide, Version 2.0. Report LBNL-43134, Lawrence Berkeley Nat. Lab, Berkeley, CA.

Vinsome, K., 1990. TETRAD User Manual. Dyad Engineering,, Calgary, Alberta, Canada.

Whitney, J. A., 1975. The effects of pressure, temperature and χ_{H_2O} on phase assemblage in four synthetic rock compositions. J. Geol. 83, 1–31.

Wisian, K. W., 2000. Insights into Extensional Geothermal Systems from Numerical Modeling. Geotherm. Resour. Council Transact. 24, 281–286.

Yano, Y., Ishido, T., 1998. Numerical Investigation of Production Behavior of Deep Geothermal Reservoirs at Super-Critical Conditions. Geothermics 27 (5/6), 705–721.

E 2002 JGR Draft Paper

This draft to be submitted to Journal of Geophysical Research in spring of 2002.

DRAFT: The onset of hydrothermal boiling: Simmering as a persistent state in hydrothermal/geothermal systems

Tom Brikowski
Geosciences Dept., University of Texas at Dallas
Richardson, TX 75083 USA, email: brikowi@utdallas.edu

Keywords: reservoir model, supercritical fluid, equation of state, reservoir simulator, software

Abstract

Simmering, or enhanced heat transport via transient vapor bubbles is a persistent state in heated H_2O systems, e.g. in household cooking. Although rarely discussed in geologic settings, simmering should be equally important and persistent in nature. Numerical modeling is used here to assess simmering in magma-hydrothermal systems using the latest NIST-standard high-temperature/pressure equation of state for H_2O embedded in the *TOUGH2* hydrothermal simulator. The models demonstrate that simmering is quite persistent in these settings owing to the development of a strong feedback between heat transport rate, fluid pressure and phase state. In freely-

convecting systems this feedback is manifested in upflow zones by P-T conditions closely paralleling the two-phase boundary on its liquid-stable side, extending to supercritical conditions along the high-pressure side of the critical isochore. At any point in the upflow zone, development of a steam phase increases pressure locally, forcing nearby points off the two-phase boundary into the liquid field in P-T space. The steam phase separates buoyantly, accumulating at any geologic traps, and eventually resorbing into the liquid. The enhanced heat transport provided by this simmering successfully dissipates most magmatic heating, and maintains the system in a "barely liquid" state for extended periods. Pressure perturbations, such as lithocap fracturing, are rapidly compensated for by the feedback process, and have only small effect, while temperature perturbations such as magma reintrusion can overcome the feedback, leading to continuous presence of vapor. The prospect that simmering may be the most common two-phase state for geologic systems has profound implications for the interpretation of mineral and vein zoning, fluid inclusions, and other geologic indicators of paleo-fluid state.

E.1 Introduction

The familiar truism that "a watched pot never boils" is a qualitative appraisal of the fact that incipient boiling (simmering, or cyclical development and convection of steam bubbles) enhances heat transport, thereby delaying or even preventing the onset of full boiling (continuously present vapor). It should not be a surprise, then, that this phenomenon may be an important aspect of two-phase convective systems in geology. Direct observation of undisturbed simmering in nature may be impossible, and therefore it is more readily investigated using numerical simulations. Significant indirect evidence for the prevalence of simmering exists in active systems and in the geologic record. In active systems the variability of steam saturation and eruptive style in geysers (*Dowden et al.*, 1991) requires transient boiling, while unexpected chemical variations during production of geothermal fields (e.g. The Geysers, CA, *Klein and Chase*, May 1995) suggests unusually transient flow fields. Injection-related low-magnitude seismic events at active geothermal systems are commonly attributed to thermal fracturing events (*Smith et al.*, 2000), but could as easily be directly related to steam bubble formation. The rock record of active and paleo-hydrothermal systems is replete with finely zoned hydrothermal minerals (*Norton et al.*, 2000) and vein fillings and selvages, generally attributed to tectonically-controlled pressure and fluid flow variations. Again these might instead have been caused by repeated changes in phase state and related pressure-temperature (PT) conditions.

Published reports of numerical models of hydrothermal and geothermal systems rarely report simmering phenomena, and none have shown simmering to be a predominant state. The results presented below demonstrate that simmering phenomena can be strongly developed in models of magmatic geothermal/hydrothermal systems when an extremely accurate fluid equation of state is employed. Episodic boiling and pressure changes on the time scale of years to decades are as readily generated by the fluid phase in these models as by rock-related factors (e.g. external tectonic or thermal contraction phenomena). The presence of

supercritical fluid conditions (T>374°C) at depth strongly encourages the development of simmering conditions higher in the system. Since simulations of combined supercritical and two-phase systems have only recently become possible, the phenomenon of simmering was evidently not encountered in earlier studies.

E.1.1 Directly Observed Supercritical Conditions in Nature

Although the brittle-ductile transition in most magmatic-hydrothermal systems is thought to be at mildly supercritical temperatures (400-500°C , e.g. *Fournier*, 1999), field observations demonstrate that the base of fluid circulation does extend to supercritical fluid conditions. These conditions (shaded region, Fig. 31) have been directly observed at depth in magmatic geothermal systems such as Kakkonda, Japan (*Ikeuchi et al.*, 1998) and Lardarello, Italy, and no doubt present in unsampled deep-circulation zones at other sites such as The Geysers, California.

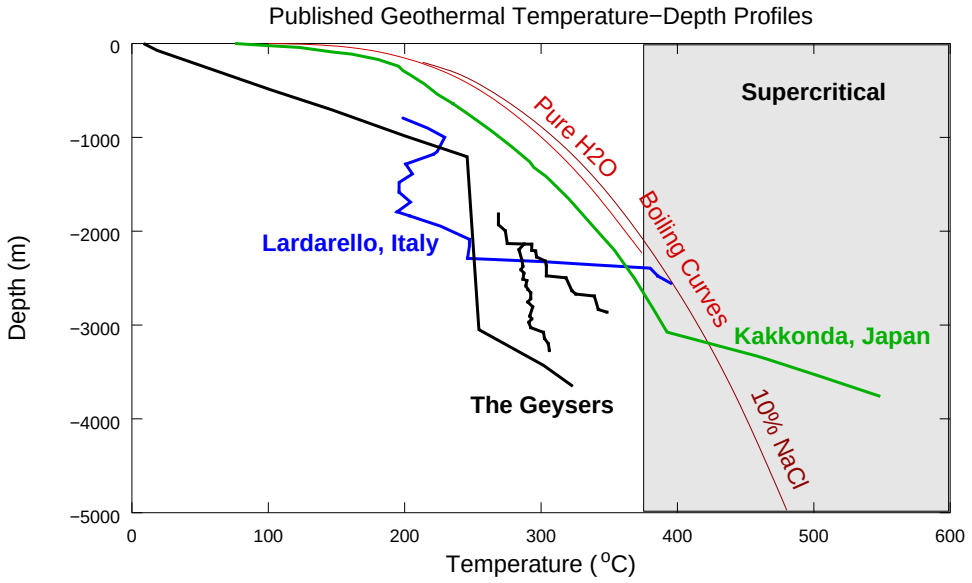

Figure 31: Temperature-depth profiles for deep geothermal systems, after *Muraoka et al.* (2000). Supercritical temperatures (shaded region) have been encountered in several deep systems, and are approached in many others.

A crucial factor in understanding the energetics of convective systems are the thermodynamic conditions at depth. When collar pressure is available, temperature-depth curves (Fig. 31) can be converted to temperature-pressure curves, which show that P-T conditions in many freely-circulating systems lie near or along the two-phase boundary ("boiling curve", Figure 32). Early production in most geothermal fields consists of "wet" steam, also reflecting natural P-T conditions along the two-phase boundary at depth. In general then, pre-production field evidence indicates many magmatic geothermal systems have PT conditions along the two-phase boundary, extending to supercritical conditions at depth in

the vicinity of the supercritical isochore (line of fluid density equal to density at the critical point, dashed line, Fig. 33).

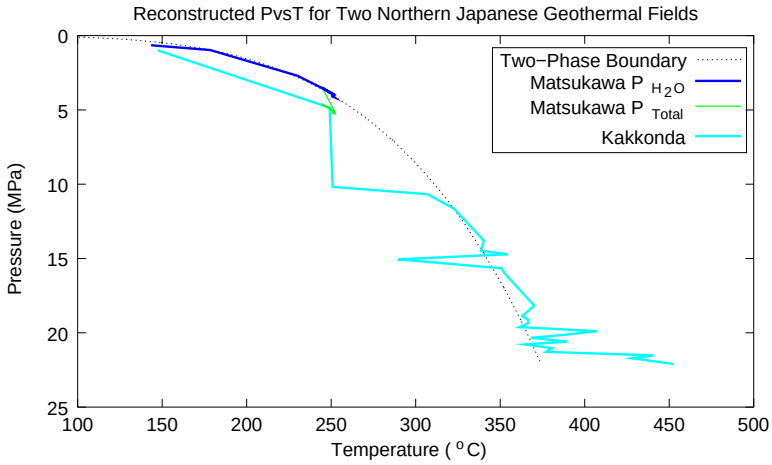

Figure 32: Temperature-Pressure depth profiles for two Japanese geothermal systems. Pressure calculated assuming pure H_2O given temperature-depth data of *Doi et al.* (1998) for well WD-1 at Kakkonda, Japan. Reconstructed P-T data for Matsukawa from *Hanano and Matsuo* (1990), who assumed pure H_2O, and corrected for P_{CO_2} ("Ptotal" line).

E.2 Supercritical Model Development

It is very difficult to study natural boiling systems directly because gaining access to them invariably perturbs conditions away from the natural state. System state as preserved in the rock record is generally known only in part, and it is particularly difficult to obtain a synoptic view from such evidence. Given these restrictions, the best way to understand the general character and development of magma-hydrothermal/geothermal systems is through numerical modeling. While a number of studies have dealt with this topic in the past, highly accurate numerical treatment of fluid properties at high temperature and pressure has only recently become possible (*Johnson and Norton*, 1991; *NIST*, 1999). In order to model the near-boiling systems described above, a high level of accuracy in determining fluid properties and state is crucial, particularly at critical and supercritical conditions in the vicinity of the magmatic heat source. There are currently few options in selecting a supercritical hydrothermal/geothermal modeling computer program. The most commonly-applied geothermal programs, *TOUGH2* (*Pruess et al.*, 1999) and *TETRAD* (*Vinsome*, 1990), are currently limited to sub-critical conditions (white area, Fig. 31). The most readily-available supercritical program (*HYDROTHERM*, *Hayba and Ingebritsen*, 1994) lacks some of the computational and gridding flexibility of *TOUGH2*. Several research codes treat liquid-only supercritical systems using finite elements (modified MARIAH, *Brikowski*, 2001b; *Brikowski and Norton*, 1989) or finite difference (FLOW6, *Norton and Hulen*, 2001), but cannot also treat boiling. Given this situation, modification of one of the above codes, particularly *TOUGH2* seemed most likely approach.

The modifications were carried out using the current international standard for computing high temperature and pressure fluid properties for pure H_2O(*NIST*, 1999). The NIST code was incorporated into the structure of the exisiting EOS1 module of *TOUGH2* to generate a supercritical EOS module "*EOS1sc*". This module serves as a plug-in conversion to allow supercritical modeling using *TOUGH2*. The supercritical equation of state module extends the range of *TOUGH2* considerably, currently giving it an applicable range of $0 < T \leq 1000$°C and $0 < P \leq 1000$ MPa. This extension allows application of *TOUGH2* to magma-hydrothermal systems, where P-T conditions at the heat source typically lie somewhere near magmatic solidus conditions (Fig. 33).

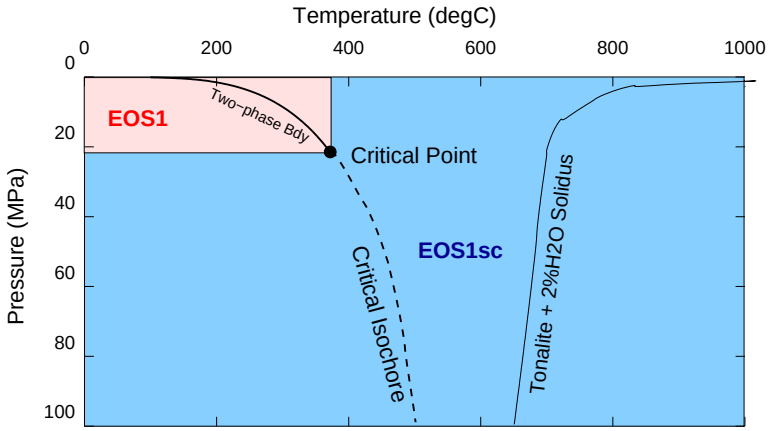

Figure 33: P-T validity range of EOS1 (white area, *Pruess et al.*, 1999) and *EOS1sc* (grey area). Liquid-vapor solidus of hydrous tonalite magma with 2 wt% H_2O shown to indicate typical magmatic conditions (*Whitney*, 1975). Dashed line shows approximate location of critical isochore (line of density equal to density at the critical point).

E.2.1 Supercritical Equation of State (*EOS1sc*)

An earlier numerical equation of state program (*Johnson and Norton*, 1991) based on the same formulation employed by the *NIST* (1999) program has been used in previous supercritical (single-phase) hydrothermal models (*Brikowski*, 2001b; *Brikowski and Norton*, 1989; *Norton and Hulen*, 2001). These applications have universally found that near-critical fluid properties have an enormous impact on the flow system. The NIST code is inherently more modular and is an international standard, and therefore was adopted for this study. Both codes are based on the same equations, which treat very accurately fluid properties and their extrema at the critical point. These extrema have a profound effect on fluid dynamics, and accurate treatment of such properties is required for accurate hydrothermal models that include the critical region. The equations use a Taylor series approximation for Helmholtz free energy outside the critical region, from which most of the remaining fluid thermodynamic properties can be obtained via numerical differentiation (*Johnson and Norton*, 1991). In the vicinity of the critical point, the non-classical *Levelt-Sengers et al.* (1983) equation for thermodynamic potential is used, which can be treated similarly to obtain fluid properties. The

equations are based on physical considerations of the internal chemistry of the fluid, and as such can be far more accurate than strictly mathematical interpolations of these properties (e.g. *International Formulation Committee*, 1967). For systems containing critical-point conditions this accuracy is fundamentally important, but it comes at a steep computational cost, since the Taylor series require calculation of many more terms at each P-T point. Verification of the proper performance of *EOS1sc* by comparison with test problems provided with the original *TOUGH2* and other examples is detailed elsewhere (*Brikowski*, 2001a,c).

E.2.2 Impact of Critical Fluid Properties

The most important fluid properties for near-critical systems are the derivatives of ρ with respect to P and T, where isobaric heat capacity $Cp = \frac{\partial \rho}{\partial T}$ and fluid expansivity $\beta = \frac{\partial \rho}{\partial P}$. Both reach theoretical values of infinity at the fluid critical point, for pure H_2O the critical point is at 374.15°C and 22.046 MPa. The extrema in these important properties for fluid movement and transport of heat and dissolved extend along the two-phase boundary from around 300°C to higher P-T along the critical isochore, or line of denisty equal to that at the critical point (Fig. 34). Systems with P-T conditions in these regions, such as those shown in Figure 32 can be expected to exhibit strong control by critical fluid phenomena.

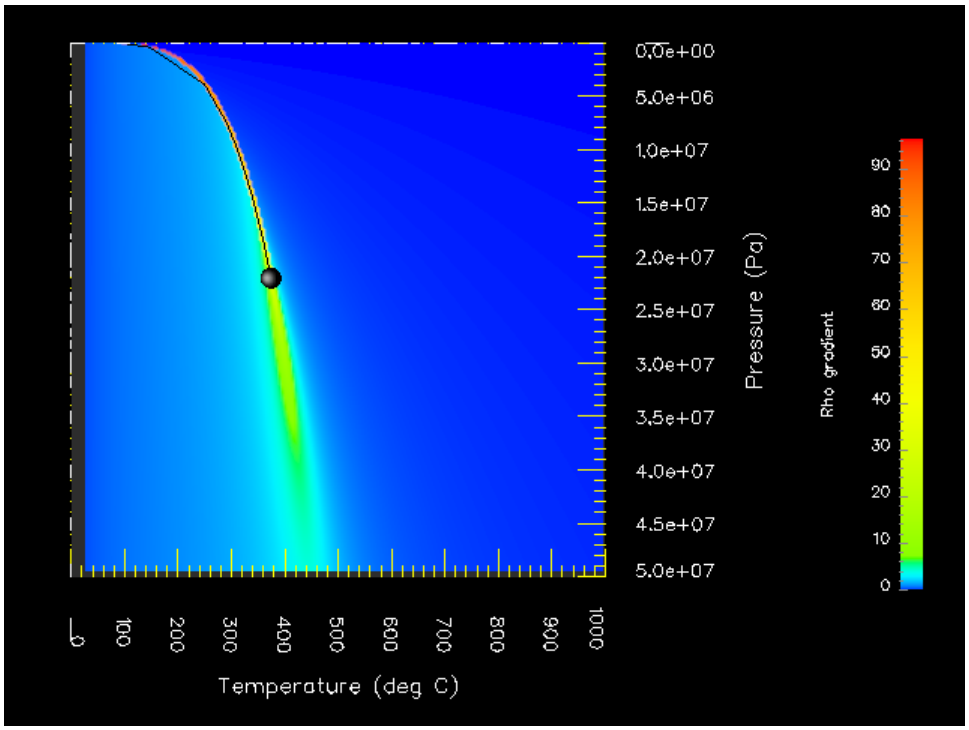

Figure 34: Density gradient vs. P and T, calculated assuming pure H_2O using NIST equation of state (*NIST*, 1999). This depicts the maximum of fluid β and Cp, which have very similar forms in the critical region. Gray line shows two-phase boundary, ending at critical point (sphere).

The principal consequence of these properties in hydrothermal systems is that P-T conditions in freely convecting systems tend to converge on the two-phase boundary and/or critical isochore. Strictly speaking, this occurs in the upflow zones where the feedback nature of convection and fluid property extrema is most influential. This tendency has been observed in many hydrothermal models that employ accurate equations of state for H_2O (*Brikowski*, 2001b; *Brikowski and Norton*, 1989; *Norton and Knight*, 1977). The feedback in the system functions by maximizing buoyancy forces (primarily dependent on horizontal density gradients, which are in turn dependent on β and Cp) in a region of minimal viscosity (resistance to flow) along the two-phase boundary and critical isochore.

In models of magma-hydrothermal systems, points in the host rock subject to warming approach the two-phase boundary or critical isochore from low temperature (Fig. 35). Buoyancy forces cause a sharp increase in velocity (convection) as the points approach the two-phase boundary, and convection limits any further increase in temperature. Conversely, points in the pluton cool toward the critical isochore, with velocity peaking sharply in the vicinity of the isochore. In this case rock permeability is generally held to be low until temperatures reach 500°C or lower, magnifying the effect of fluid property extrema along the critical isochore. Portions of the system attempting to depart from this zone of maximum density gradient experience reduced convection. Above the pluton, points depressurizing above the two-phase boundary don't heat as rapidly, and move left on the P-T diagram back into the region of maximum buoyancy. Similarly pluton points cooling beyond the critical isochore experience reduced convection, and cool more slowly, eventually moving to the right on the PT diagram back into the region of maximum convection along the critical isochore. Forced convection systems (externally controlled vertical pressure gradient) may show other P-T distributions, but upflow zones in freely convecting systems will tend toward the two-phase boundary/critical isochore.

A numerical problem that arises from the fluid property extrema is that in the vicinity of the critical point, fluid density changes so rapidly that only small time steps can be taken. In particular, mass balance equations in fluid flow simulators make use of the divergence, stating that for each control volume (finite element or finite difference node):

$$\underbrace{\frac{\partial \rho}{\partial t}}_{\text{Content}} = \underbrace{\nabla \cdot (\rho \cdot \vec{q})}_{\text{Boundary Fluxes}} \tag{7a}$$

$$= \nabla\rho \ + \ \rho(\nabla_{\mathrm{PT}} \cdot \vec{q}) \tag{7b}$$

where $\vec{q}$ is the Darcy velocity, and a two-dimensional case is assumed. In other words, that the sum of mass fluxes across the boundary of the control volume is equal to the change in mass content of that volume. Since T and P are (locally) single-valued functions of xy (7b) can be rewritten as

$$\frac{\partial \rho}{\partial t} = \frac{\partial \rho}{\partial T} + \frac{\partial \rho}{\partial P} + \rho(\nabla \cdot \vec{q}) \tag{8}$$

In the vicinity of the critical point the terms on the right-hand side of (8) approach infinity, and begin to severely violate the equality. Numerical simulators limit the magnitude of these

violations, typically by reducing time steps until the error in mass balance (i.e. sum of left and right sides of Eqn. 8) falls below a user-set criterion. In this way, timesteps will typically decrease to well under one year in magma-hydrothermal simulations containing near-critical fluids, posing a severe problem for models attempting to span tens or hundreds of thousands of years. It is important to note that choice of energy state variables (e.g. T or enthalpy) does not affect the occurence of this problem. Any simulator that makes use of volume averages must employ density as the mass balance variable, and will therefore encounter this timestep problem in the critical region.

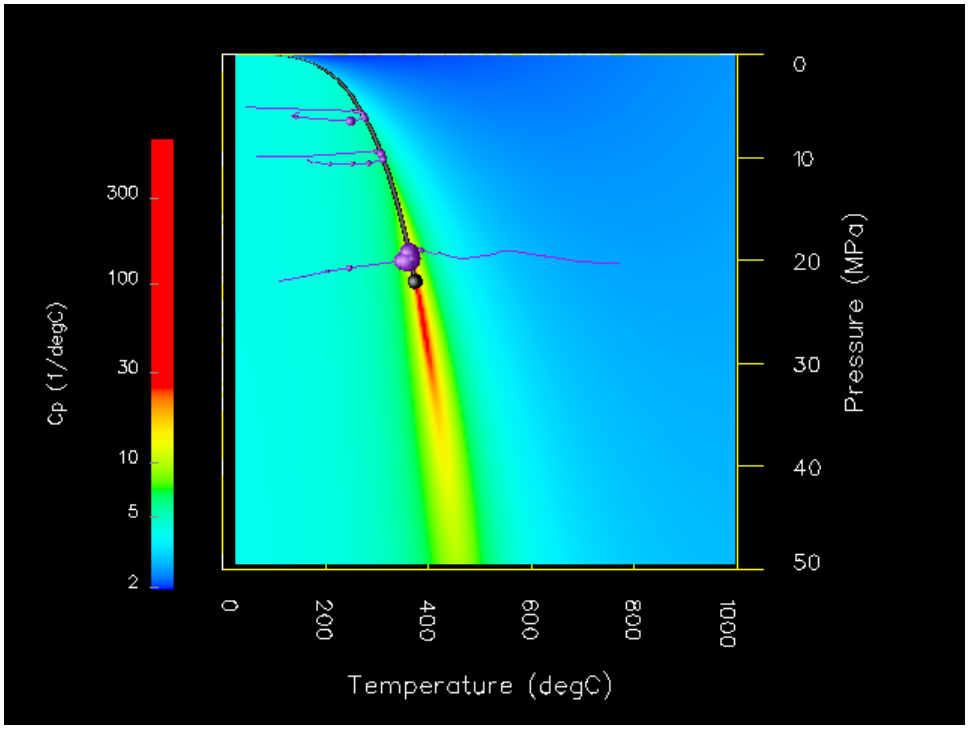

Figure 35: P-T paths (purple lines) for selected points, showing velocity magnitude (filled circles, size proportional to velocity magnitude) for prograde heating of system. Density gradient shown by color (represented here by Cp). Velocity is large only in the vicinity of the two-phase boundary and critical isochore.

E.3 Simmering in Geothermal/Hydrothermal Systems

E.3.1 Process Description

Simmering in porous media is a complex feedback process between convection and phase change (and associated perturbations in fluid pressure and convection rate). This phenomena will develop in systems that are freely convecting, and consequently that can adjust pressure distribution throughout the system in response to changes in convection and phase distribution. In magma-hydrothermal systems, a simmering zone should develop above the

pluton, its height and thickness determined by the pre-intrusion temperature distribution ("preheating") and presence or absence of a caprock.

The simmering process can be illustrated using a hypothetical plutonic setting, patterned after the pre-heated pluton intrusion with caprock scenario of *Hayba and Ingebritsen* (1997) (Fig. 36). Pressure-temperature paths for the three points indicated in Figure 36 were

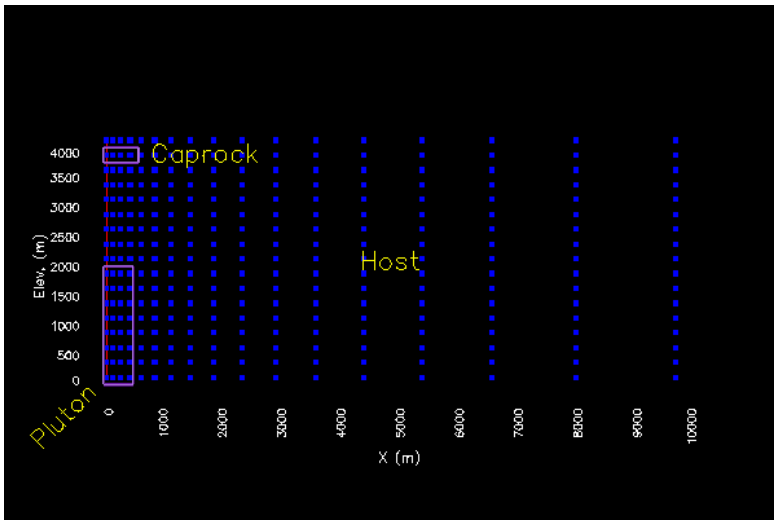

Figure 36: Computational grid and lithologic zones for hypothetical system of caprock, host rock and pluton. Models will use caprock permeability as $1.0\text{x}10^{-18}$ m^2, host rock $1.0\text{x}10^{-15}$ m^2, and pluton as $5.0\text{x}10^{-17}$ for temperatures less than the critical point. Monitoring points for P-T (magenta lines in Fig. 35 shown by magenta circles. Profile line used in subsequent figures show in red.

illustrated in Figure 35. In this system, a vertical pressure temperature profile similar to the observed profiles shown in Figure 32 show rapid evolution toward the two-phase boundary, with conditions nearing critical at the top of the pluton (i.e. by 2000 yrs, Fig. 37).

When viewed in detail, the PT history at a point is considerably more complicated than indicated in Figure 37. Examining one point at each time step, over a period of about 100 years shows that the point oscillates on and to the high P side of the two-phase boundary in a roughly elliptical path (Fig. 38). Each point in the upflow zone undergoes a similar cycle, a point 250 m below the lithocap is illustrated. The point gradually migrates to lower pressures and temperatures along the two-phase boundary, interrupted by periods of retrograde motion on the liquid side of the boundary. The bold line illustrates a single cycle, from disappearance of steam at this point (cell "C" in the inset, Fig. 38, to the return of steam at that point 19 years later. The beginning of the cycle is designated at the time steam disappears from cell C ("C Condenses"). Pressure increases rapidly, ceasing when C's top neighbor cell A condenses one year after the start of the cycle. From that point a period of steady flow at C persists for 16 years, while steam steadily accumulates at the base of the lithocap in cell B, and C gradually heats and depressurizes toward the two-phase

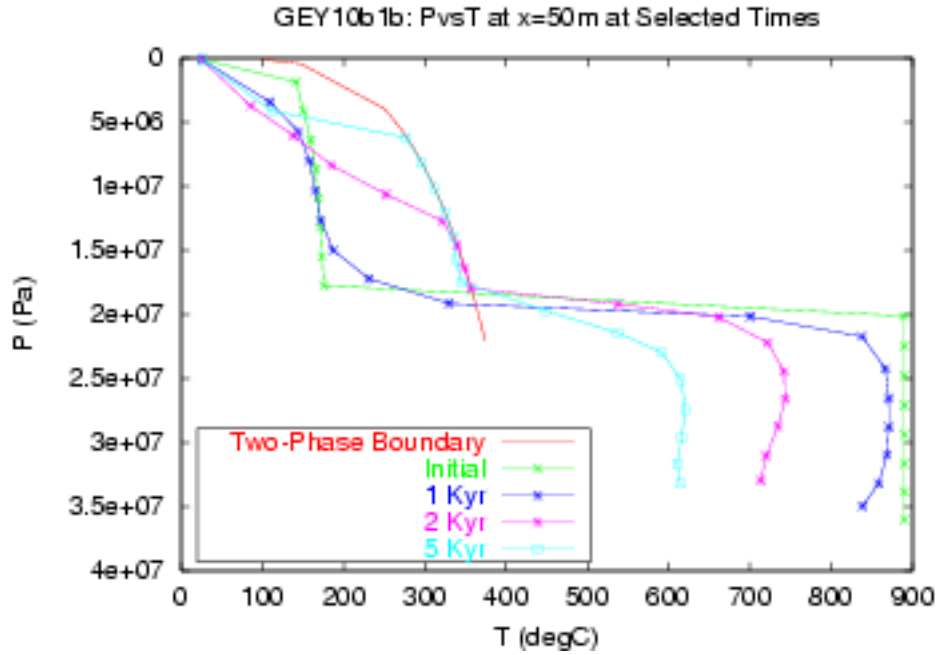

Figure 37: PT profiles along x=50m at selected times

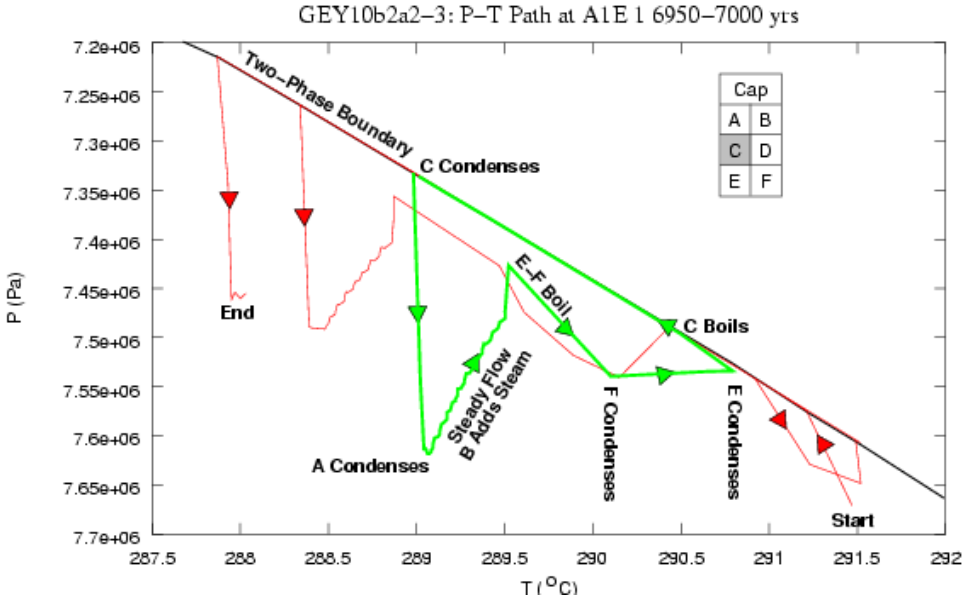

Figure 38: PT history for 100 years at (x,y)=(50,3375)m

boundary. Then pressure and temperature increase rapidly for half a year when C's bottom neighbors E and F boil. This is caused by greatly increased mass flux (via steam) from E to C, and increase in pressure in E. When the steam in F is resorbed, C heats isobarically toward the two-phase boundary for 1/4 year. When steam leaves F, C reaches saturation, and saturation increases while C moves up the two-phase boundary to begin another cycle. This is the feedback process in extreme detail. Enhanced phase separation at the point of interest (cell C) encourages cooling, driving C into the liquid state. Simultaneously boiling above C, encouraged by steam migration out of C decrease convection, and cause isothermal pressure increase. Reversion of these cells to liquid allows incresed convection, leading to heating and depressurization as a steady flow field is reestablished. Boiling in cells below C increase pressure and heating, driving C back to the two-phase boundary.

Less obvious from the P-T diagram (Fig. 38) is the separation and accumulation of steam at the base of the lithocap. In a slighly different example, with a 1km thick lithocap (meant to simulate conditions at The Geysers, California) steam develops at the base of the upflow zone (an area with up to 80% steam saturation) and migrates rapidly upward (Fig. 39). The migration rate is approximately the same as the steam pore velocity in the model, i.e. steam bubbles migrate through the system to accumulate at the lithocap. This accumulation grows for 6-10 years, then gradually shrinks to zero saturation via resorbtion over another 10-15 years. This is precisely how a simmering system should behave. Enhanced heat transport via the formation of a transient, mobile steam phase dissipates heat entering the base of the upflow zone. Cooling at the top of the upflow zone, in this case the base of the lithocap, eventually causes that steam to resorb.

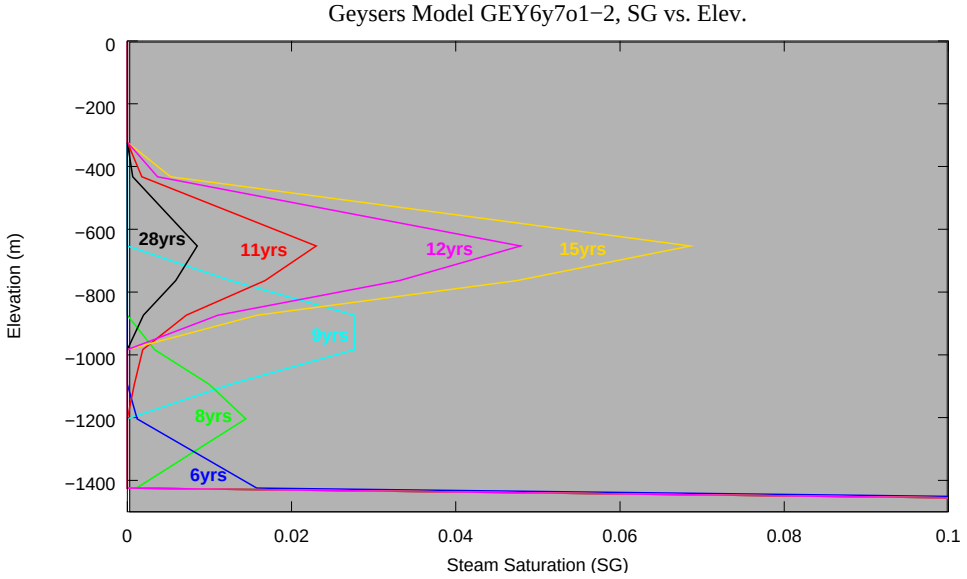

Figure 39: Steam saturation (SG) profiles at x=4935m for sequential times, showing advection of steam bubbles upward with flow field. This example from preliminary models of boiling at The Geysers geothermal field (*Brikowski*, 2001a).

E.3.2 Persistence

Why does simmering persist? Enhanced heat transport by transient steam bubbles dissipates basal heating efficiently (Fig. 40). For the same system portrayed in Figure 39, it is evident that enhanced heat transport by the steam phase (at around 25775 system years, or at the 12-year point shown in Fig. 39 and the top of 40) raises temperatures at the base of the lithocap. As these temperatures decline via conductive cooling steam saturation declines, and by cycle time 30 years steam disappears, heat flow declines, and temperature begins a slow steady decline until the next steam pulse arrives.

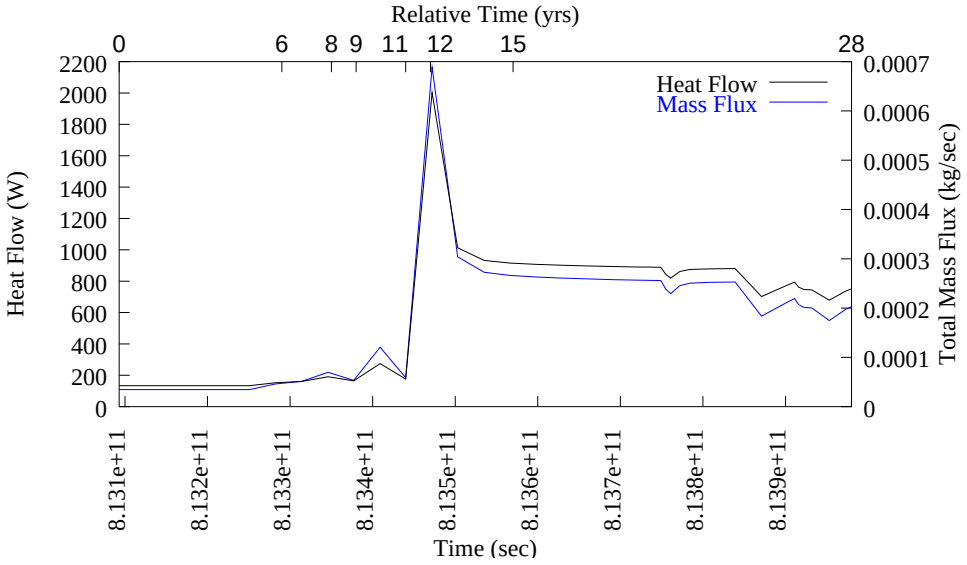

Figure 40: Heat Flux vs. Time at base of lithocap for model shown in Figure 39. Development of mobile steam phase greatly enhances heat transport, allowing the system to come into equilibrium with basal heating via conductive flux from an underlying magma.

Just as in cooking, the only way to push the system into maintaining a high, steady steam saturation is to greatly increase basal heating (e.g. reintrusion), with or without pressure release at the top (caprock fracturing).

E.3.3 External Controls vs. Simmering

As described above, the process of hydrothermal simmering can readily provide the fine scale pressure-temperature variations responsible for observed zonation of minerals and veins in the rock record, deep seismic noise and discharge variations in present day systems. These phenomena are traditionally attributed to non-convective processes such as tectonic fracturing and depressurization or reintrusion of magma. Implicit in the results above is that a vapor-dominated state is at best highly transient for the simple models envisioned. Since vapor-dominated conditions are clearly present in settings such as The Geysers geothermal system in California, a more complicated scenario is required. As noted by *Hayba*

and Ingebritsen (1997); *Ingebritsen and Sorey* (1988) and many others, a low-permeability caprock is generally required to develop a significant concentration of steam. Many of these same authors postulate tectonic fracturing and depressurization as crucial in forming vapor-dominated conditions. This is not borne out in simmering models; the pressure/saturation feedback process adjusts quickly to fracturing in the caprock, and increased steam saturation related to the fracturing is short-lived. When viewed in P-T space, the point in the upflow zone immediately below the caprock moves rapidly to lower pressure along the two phase boundary (boils), and then experiences the familiar retrograde P-T cycles (Fig. 38) then cools back into the liquid field 50 years after fracturing (blue line, 41). The neighboring cell beneath the lithocap (cell "B" of Fig. 38) experinces steam saturations up to 20% after fracturing, but again this persists for only 50 years. Immediately following the fracturing event, points in the upflow zone adjust upward along the two-phase boundary, but primarily remain liquid-saturated. Only in the case of frequently repeated fracturing could this process result in development of a steady steam zone ("full boiling"), but saturations never exceed 25% in the model system.

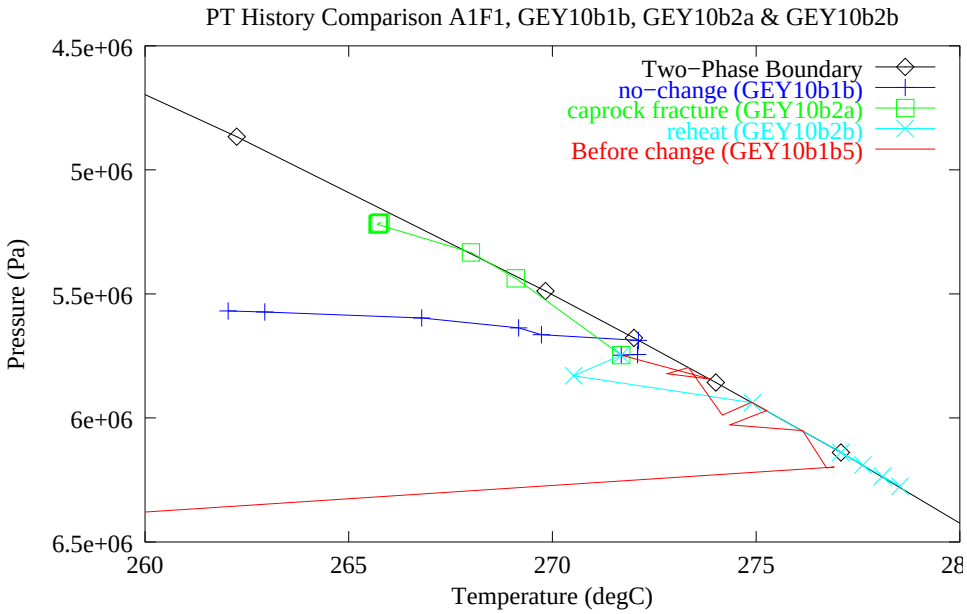

Figure 41: Simmering system response to caprock fracture (blue line) and magma reintrusion (magenta line). Cyan line shows PT path of point in upflow zone immediately below lithocap (cell "A" of inset, Fig. 38). Green line shows evolution of this point if no changes made in the system.

A second possibility for generation of vapor-dominated conditions is reheating of the system (reintrusion). *Hayba and Ingebritsen* (1997) found this to be the only effective means of generating such conditions, although they did not consider the case of caprock fracture. In the case of reheating, points in the upflow zone move to higher P-T along the two-phase boundary. Cell A remains two-phase (magenta line, Fig. 41), steadily increasing until reaching full steam saturation. Simmering still persists at depth, but steam accumulates rapidly

beneath the lithocap. This process appears far more likely to be responsible for generation of vapor-dominated conditions in geothermal systems. In fact this is conceptually reasonable. In a freely convecting (highly permeable) system, pressure should adjust very rapidly throughout the system, quickly damping out the effects of perturbations. Temperature, or heat perturbations are much longer lasting because they also involve the rock matrix, and therefore are more likley to cause state changes in the system (e.g. drive it to vapor dominated conditions).

E.3.4 Simmering as a novel process

Considering that simmering is a process observed on an almost daily basis in the home, it is surprising to find that it has recieved little discussion as a formal geological process. As demonstrated above, simmering in hydrothermal systems is a remarkably persistent state *once it has been initiated*. The *EOS1sc* module used in this study is the first extremely accurate supercritical equation of state to be employed in multiphase convective modeling in geology. Application of this module allows accurate models extending from shallow two-phase zones down to magmatic conditions. The models described above, as well as earlier liquid-only supercritical models have made it clear that the deepest portions of hydrothermal/geothermal flow systems reside near the critical point of the fluid. In a model that assumes atmospheric conditions at the surface, having near-critical conditions at the base of the flow system implies vertical P-T profiles sub-parallel to the two-phase boundary/critical isochore. Such conditions in a freely convecting system (i.e. with sufficient permeability and lacking in flow-limiting heterogeneity) appear to be sufficient to drive the system to a simmering state. Although this phenomenon was first encountered in a supercritical model using *EOS1sc*, standard *TOUGH2* models (using the subcritical EOS1 equation of state) yield the same simmering behavior when the subcritical portion of the *EOS1sc* results are used as an initial condition (Fig. 42). Without the application of *EOS1sc*, P-T profiles sub-parallel to the two-phase boundary would not be recognized as typical, and therefore apparently have been avoided by most workers. It must be emphasized that critical conditions at depth are not required to yield a system that simmers, they only make it easier to encounter such conditions as the model progresses. *EOS1sc* allows determination of realistic basal boundary conditions for subcritical models, which drives those models into heretofore-avoided areas.

E.4 Summary

Simmering (incipient boiling), a familiar household phenomenon, may be a common feature in geothermal/hydrothermal systems. If so, our views may need revision as to the meaning of phase-state indicators in the rock record, behavior of present-day two-phase convective systems (i.e. magmatically-heated geothermal fields), and numerical simulations of such systems that do not exhibit simmering. Similarly, fine-scale variations in hydrothermal mineral composition (zoning), veining, low-magnitude seismic activity in active systems, variability in natural and extracted geothermal fluids all are consistent with the activity of the simmering process at depth. While supercritical conditions are not reqired at depth to

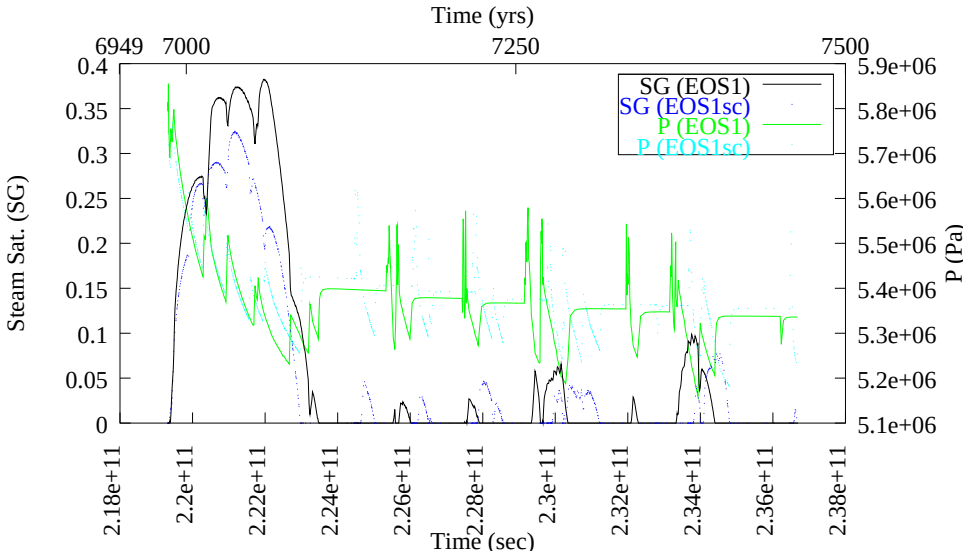

Figure 42: Comparison of EOS1 and *EOS1sc* simmering results for cell "B" (inset of Fig. 38). Diagram begins at the same time as that figure, extending for 500 years. These models consider only cells with subcritical temperatures (i.e. near-critical cells form the bottom boundary). Differences result from near-critical fluid property differences in the two routines.

generate a simmering state, they increase the likelihood simmering will be encountered in models or in the system itself. And finally, if supercritical modeling is attempted, it should make use of the most accurate possible equations of state for the fluid. The models discussed in this paper were carried out using such an equation of state, distributed as a worldwide standard by the U.S. NIST, and adapted here for use with the geothermal reservoir simulator *TOUGH2*. Application of highly accurate tools such as this can reveal crucial details about natural systems that, while seemingly obvious in retrospect, were not previously recognized as important. Simmering as the predominant heat transport mechanism in high-temperature hydrothermal and geothermal systems is one such process.

Acknowledgments

This research supported by U. S. Dept. of Energy grant DE-FG07-98ID13677 to UTD, with subcontracts to David Blackwell of SMU and Denis Norton, consultant, Stanley ID. Their contributions to the conceptual aspects of this software development and application have been crucial. James Johnson of LLNL provided the source code for early versions of the supercritical equation of state. Karsten Pruess provided encouragement throughout this development. Invaluable testing of successive versions of *EOS1sc* was carried out by Ken Wisian of SMU.

References

Brikowski, T. H., Modeling supercritical systems with tough2: The eos1sc equation of state module and a basin and range example, in *Geother. Resources Council Transact.*, vol. 25, pp. 285–289, Geothermal Resources Council, Davis, CA, 2001a.

Brikowski, T. H., Deep fluid circulation and isotopic alteration in the geysers geothermal system: Profile models, *Geothermics*, *30*, 333–47, 2001b.

Brikowski, T. H., Modeling supercritical systems with tough2: Preliminary results using the eos1sc equation of state module, in *Proceedings: Twenty-Sixth Workshop on Geothermal Reservoir Engineering*, vol. 26 of *SGP-TR-168*, p. 8, Stanford University, Stanford, CA, 2001c.

Brikowski, T. H., and D. Norton, Influence of magma chamber geometry on hydrothermal activity at mid-ocean ridges, *Earth Planet. Sci. Lett.*, *93*, 241–255, 1989.

Doi, N., O. Kato, K. Ikeuchi, R. Komatsu, S. I. Miyazaki, K. Akaku, and T. Uchida, Genesis of the plutonic-hydrothermal system around quaternary granite in the kakkonda geothermal system, japan, *Geothermics*, *27*, 663–690, 1998.

Dowden, J., P. Kapadia, G. Brown, and H. Rymer, Dynamics of a geyser eruption, *J. Geophys. Res.*, *96*, 18,059–72, 1991.

Fournier, R. O., Hydrothermal processes related to movement of fluid from plastic into brittle rock in the magmatic-epithermal environment, *Econ. Geol.*, *94*, 1193–1211, 1999.

Hanano, M., and G.-I. Matsuo, Initial state of the matsukawa geothermal reservoir: Reconstruction of a reservoir pressure profile and its implications, *Geothermics*, *19*, 541–560, 1990.

Hayba, D. O., and S. E. Ingebritsen, The computer model hydrotherm, a three-dimensional finite-difference model to simulate ground-water flow and heat transport in the temperature range of 0 to 1,200 degrees c, *Wri 94-4045*, U. S. Geol. Survey, Denver, CO, 1994.

Hayba, D. O., and S. E. Ingebritsen, Multiphase groundwater flow near cooling plutons, *J. Geophys. Res.*, *102*, 12,235–12,252, 1997.

Ikeuchi, K., N. Doi, Y. Skagawa, H. Kamenosono, and T. Uchida, High-temperature measurements in well wd-1a and the thermal structure of the kakkonda geothermal system, japan, *Geothermics*, *27*, 591–607, 1998.

Ingebritsen, S. E., and M. L. Sorey, Vapor-dominated zones within hydrothermal systems: Evolution and natural state, *J. Geophys. Res.*, *93*, 13,635–13,655, 1988.

International Formulation Committee, *A formulation of the thermodynamic properties of ordinary water substance*, IFC Secretariat, Düsseldorf, Germany, 1967.

Johnson, J. W., and D. Norton, Critical phenomena in hydrothermal systems: State thermodynamic, electrostatic, and transport properties of h_2o in the critical region, *Am. J. Sci.*, *291*, 541–648, 1991.

Klein, C., and D. Chase, Chemical transients during production of high gas wells at the northern geysers steam field, ca, usa, *World Geothermal Congress*, *3*, 1641–1645, May 1995, iSBN 0-473-03123-X.

Levelt-Sengers, J. M. H., B. Kamgar-Parsi, F. W. Balfour, and J. V. Sengers, Thermodynamic properties of steam in the critical region, *J. Phys. Chem. Ref. Data*, *5*, 1–51,

1983.

Muraoka, H., K. Yasukawa, and K. Kimbara, Current state of development of deep geothermal resources in the world and implications to the future, in *Proceedings of the World Geothermal Congress 2000*, edited by E. Iglesias, D. Blackwell, T. Hunt, J. Lund,, and S. Tmanyu, pp. 1479–1484, International Geothermal Association, 2000.

NIST, Nist/asme steam properties database: Version 2.2, *NIST Standard Reference Database 10*, U.S. National Institute of Standards and Testing, 1999.

Norton, D., and J. Knight, Transport phenomena in hydrothermal systems: Cooling plutons, *Am. J. Sci.*, *277*, 937–981, 1977.

Norton, D., J. Hulen, and B. Dutrow, Patterns of dynamical hydrothermal activity in geothermal resources, 2000, special Progress Note, submitted to U.S. DOE Office of Geothermal and Wind Technologies.

Norton, D. L., and J. B. Hulen, Geologic analysis and thermal-history modeling of the geysers magmatic-hydrothermal system, *Geothermics*, *30*, 211–234, 2001.

Pruess, K., C. Oldenburg, and G. Moridis, Tough2 user's guide, version 2.0, *Report LBNL-43134*, Lawrence Berkeley Nat. Lab, Berkeley, CA, 1999.

Smith, J. L. B., J. J. Beall, and M. A. Stark, Induced seismicity in the se geysers field, *Geotherm. Resour. Council Transact.*, *24*, 331–336, 2000.

Vinsome, K., *TETRAD User Manual*, Dyad Engineering,, Calgary, Alberta, Canada, 1990.

Whitney, J. A., The effects of pressure, temperature and $\chi_{\mathrm{h_2o}}$ on phase assemblage in four synthetic rock compositions, *J. Geol.*, *83*, 1–31, 1975.